IEEE Access
Multidisciplinary ⋮ Rapid Review ⋮ Open Access Journal

Received 5 September 2022, accepted 23 September 2022, date of publication 27 September 2022, date of current version 7 October 2022.

Digital Object Identifier 10.1109/ACCESS.2022.3210260

RESEARCH ARTICLE

Wavelet Interval Type-2 Takagi-Kang-Sugeno Hybrid Controller for Time-Series Prediction and Chaotic Synchronization

DUC-HUNG PHAM[1,2], CHIH-MIN LIN[2], (Fellow, IEEE), VAN NAM GIAP[3], TUAN-TU HUYNH[4], (Member, IEEE), AND HSING-YUEH CHO[2]

[1]Faculty of Electrical and Electronic Engineering, Hung Yen University of Technology and Education, Hai Duong 160000, Vietnam
[2]Department of Electrical Engineering, Yuan Ze University, Taoyuan 320, Taiwan
[3]School of Electrical & Electronic Engineering, Hanoi University of Science and Technology, Hai Ba Trung, Hanoi 100000, Vietnam
[4]Faculty of Mechatronics and Electronics, Lac Hong University, Bien Hoa 810000, Vietnam

Corresponding authors: Chih-Min Lin (cml@saturn.yzu.edu.tw) and Duc-Hung Pham (duchung.pham@utehy.edu.vn)

This work was supported by the Ministry of Science and Technology of Republic of China under Grant MOST 109-2221-E-155-027-MY3.

ABSTRACT This paper presents a new hybrid neural network controller for time series prediction and chaotic synchronization. The proposed controller is called as a wavelet interval type-2 Takagi-Kang-Sugeno (TSK) fuzzy brain emotional learning cerebellar model articulation controller (WIT2TFBCC), and it consists of a wavelet interval type-2 TSK fuzzy brain emotional learning controller (WIT2TFBELC), and a wavelet interval type-2 TSK fuzzy cerebellar model articulation controller (WIT2TFCMAC). The proposed WIT2TFBCC can serve both as a control signal for chaotic master-slave synchronization and as a prediction output signal for the time series predictor. Moreover, a robust compensator is used to achieve robust ability of the system. A Lyapunov function was used to establish the adaptive laws and effectively adjust the system parameters online. Finally, two examples of the application are presented to illustrate the performance of proposed method.

INDEX TERMS TSK fuzzy system, interval type-2 wavelet function, brain emotional learning control, cerebellar model articulation controller, 5D chaotic system, Henon map time series.

I. INTRODUCTION

Prediction of chaotic time series is always a major problem in control engineering when dealing with unknown phenomena with multiple variables in nonlinear systems and time-varying systems [1]. Prediction has many applications in various fields of science, such as medicine [2], economics [3], COVID-19 pandemic [4], and especially in engineering [1], [5], [6], [7]. Chandra *et al.* [8] recommended a hybrid deep learning methods using convolutional neural networks, providing another comparison with simple neural networks that use stochastic gradient descent and adaptive moment estimation (Adam) for training. Li *et al.* [9] presented an echo state network with improved topology for accurate and efficient time series prediction.

The associate editor coordinating the review of this manuscript and approving it for publication was Min Wang.

Furthermore, many studies using the chaotic trajectory synchronization have been published in recent years, such as Giap *et al.* presented a 3D Lorentz chaos system for secure transmission [10], The applications of synchronization of chaotic systems for the secure communication can be found in [11], [12], and [13]. Lin *et al.* recommended a 4D memristive chaos synchronization for image encryption [14]. Recently, a multilayer type-2 fuzzy control system was discussed for the synchronization of 5D nonlinear chaotic systems [15]. Hosny *et al.* introduced a 4D hyperchaotic Chen system for color image encryption [16]. Yan *et al.* presented a 5D fractional chaotic system synchronization, which could be a good choice for secure transmission [17]. A type-2 BELC was proposed for 3D Lorentz chaotic systems [18]. Huynh *et al.* introduced the wavelet type-2 fuzzy brain imitated neural network for the synchronization of 3D chaotic systems [19]. The synchronization of chaotic systems by using electronic components can be found in [20].

In fuzzy systems, there are generally two types, namely Takagi- Sugeno- Kang (TSK) fuzzy systems (FS) and Mamdani-Larsen fuzzy systems [21]. In the TSKFS, the introductory parts of the TSK rules are similar to the ''IF'' part of the other fuzzy inference (FI) rules. And the ''THEN'' part of the TSK rules is generally a polynomial function of the input variable. This means that the constant in a general inference process is replaced by the linear local equation in the previous parts of a TSK -based FI model. This makes it more expressive than the basic FI models. Therefore, the TSK fuzzy inference model can improve mapping and achieve accurate approximation performance, which makes it more powerful for various applications. Therefore, in this work, we combined TSK with CMAC and BELC channels to develop a new controller, the wavelet interval type-2 TSK fuzzy brain emotional learning cerebellar model articulation controller (WIT2TFBCC).

To date, type-1 and type-2 intelligent control systems based on fuzzy inference systems (FIS) have developed rapidly in many fields [22], [23]. Since the type-1 FIS (T1FIS) relies on fixed membership functions, it cannot efficiently deal with the uncertainties of the inputs and parameters of nonlinear systems. To overcome this problem, type-2 fuzzy inference systems (T2FIS) and interval type-2 FIS (IT2FIS) are generally used because they are more general than T1FIS, have greater design freedom to achieve better control performance, and improve the response to the input uncertainty of membership functions. Nevertheless, deciding the membership functions and network dimension for T2FIS and IT2FIS is certainly a difficult task. The trial-and-error approach is a common way to constrain the network structure dimension, but it usually takes a lot of time to train and learn and does not guarantee that the parameters and network structures can be precisely defined. For this reason, many studies have developed solutions that combine various effective techniques, additional networks and algorithms such as wavelet function [7], [22], function link network [24] and self-organising algorithms [22].

Due to the imprecision of system uncertainties and external disturbances, nonlinear chaotic synchronization systems always pose a challenge to researchers. To solve these problems, Lucas *et al.* [25] developed the Brain Emotional Learning Controller (BELC). BELC is comprised of sensory input, sensory learning, sensory output, emotional input, emotional learning, emotional output, and output from the controller. BELC has been integrated with another system in order to boost its performance, such as CMAC [12], fuzzy system [13], TSK fuzzy system [14], type-2 fuzzy system [18], and wavelet type-2 fuzzy system [19]. BELC has been utilized for chaotic synchronization and secure communication [12], [13], [14].

The proposed method has combined the advantages of wavelet interval type-2 function with TSKFS to form a neural network (NN) structure for brain emotion learning. The simulation of Henon chaotic time series prediction and the simulation of 5-D hyperchaotic synchronization illustrate the performance of our proposed method. Subsequently, the proposed method can be extended and applied to other electromechanical underactuated systems such as [26], [27], and [28]. The main contributions of this work are listed below:

(1) A new wavelet IT2FIS will be added to the BELC and CMAC channels to improve response to member function input uncertainty.

(2) TSKFS for dual-channel CMAC and BELC to update parameters more flexibly, improve mapping, and provide accurate approximation performance.

(3) A proposed WIT2TFBCC controller is designed for chaotic system synchronization and prediction system.

(4) Using Lyapunov stability theory to prove the stability of the proposed system.

The content of this paper consists of the following parts: Section I introduces the problem to be solved, Section II presents the proposed WIT2TFBCC for synchronization of chaotic systems and shows how the update of the controller parameters is determined by the Lyapunov method, Section III shows the proposed WIT2TFBCC for time series prediction and demonstrates the stability of the proposed method. Section IV presents the numerical simulation results for 5-D hyperchaotic in Matlab software. Section V shows the result of Henon map time series prediction. Finally, section VI presents the conclusion of the paper. The main differences of the proposed controller from others are listed in Table 1.

II. WAVELET INTERVAL TYPE-2 TAKAGI-SUGENO-KANG FUZZY BRAIN EMOTIONAL CEREBELLAR MODEL ARTICULATION CONTROLLER (WIT2TFBCC)

Consider a novel 5D hyperchaotic system expressed as [29]

$$\begin{cases} \dot{x}_1 = a_1 x_2 + a_2 x_4 \\ \dot{x}_2 = -a_1 x_1 - a_2 x_1 x_4 \\ \dot{x}_3 = a_3 x_4 \\ \dot{x}_4 = -a_2 x_1 x_2 - a_4 x_3 \\ \dot{x}_5 = -a_3 x_1 \end{cases} \tag{1}$$

where a_1, a_2, a_3 and a_4 can be exactly known, and the slave system can be provided as:

$$\begin{cases} \dot{y}_1 = a_1 y_2 + a_2 y_4 + \Delta Y(y_1) + n_{d1} + u_1 \\ \dot{y}_2 = -a_1 y_1 - a_2 y_1 y_4 + \Delta Y(y_2) + n_{d2} + u_2 \\ \dot{y}_3 = a_3 y_4 + \Delta Y(y_3) + n_{d3} + u_3 \\ \dot{y}_4 = -a_2 y_1 y_2 - a_4 y_3 + \Delta Y(y_4) + n_{d4} + u_4 \\ \dot{y}_5 = -a_3 x_1 + \Delta Y(y_5) + n_{d5} + u_5 \end{cases} \tag{2}$$

where $\boldsymbol{u} = [u_1, u_2, u_3, u_4, u_5]^T$ is the control input vector, $\boldsymbol{n}_d = [n_{d1}, n_{d2}, n_{d3}, n_{d4}, n_{d5}]^T$ is the unknown external disturbance, $\Delta \boldsymbol{Y}(\boldsymbol{y}) = [\Delta Y(y_1), \Delta Y(y_2), \Delta Y(y_3), \Delta Y(y_4), \Delta Y(y_5)]^T$ is the uncertainty of the system, and $y_i (i = 1, 2, 3, 4, 5)$ is the slave state. The tracking error can be

TABLE 1. The main differences of the proposed controller from other methods.

	Method	The main structure and its application	Additional techniques	Membership function	System weights	Mathematical solution method to determine the adaptive learning laws and convergence analysis
1	Our method	Consisting of one CMAC, one BELC, two wavelet interval type-2 TSK fuzzy inference systems (one can be used for BELC and one for CMAC).	Consisting of SMC to design the adaptive laws	Consisting of the wavelet type-2 function	Consisting of wavelet interval type-2 TSK fuzzy adaptive weights that can be updated online by adaptive laws. And consisting of relative coefficient weights of two subnetworks (CMAC and BELC) that can also be updated by adaptive laws.	Consisting of a Lyapunov function.
2	WTSKFCMAC [7]	Comprising TSK fuzzy rules, a CMAC	Consisting of SMC to design the adaptive laws	Consisting of the Gaussian function	Consisting of adaptive weights	Consisting of a Lyapunov function
3	RCFBC [12]	Comprising a fuzzy inference system, a BELC, a RCMAC and it can be acted as a main controller	Consisting of SMC to design the adaptive laws	Consisting of the Gaussian function	Consisting of adaptive weights	Consisting of a Lyapunov function
4	T2HC [30]	Comprising a Type-2 fuzzy inference system, a Type-2 fuzzy CMAC, a BELC, and it can be acted as the main controller.	Consisting of sliding mode controller.	Consisting of the Gaussian function	Consisting of adaptive dynamic weights	Consisting of a Lyapunov function.
5	IT2RFRBF [31]	Comprising an interval type-2 recurrent neural network.	None	Consisting of the ellipsoidal membership function	Consisting of adaptive weights	Consisting of a Lyapunov function
6	AORTC [32]	Comprising a CMAC, a TSK fuzzy membership function and it can be acted as a main controller	Consisting of back-stepping control technique to design the adaptive laws	Consisting of the type-2 fuzzy elliptic membership function	Consisting of adaptive weights by TSK fuzzy membership function	Consisting of a Lyapunov function
7	RWBEL [33]	Comprising a BELC ,a RNN, and it can be acted as a main controller	Consisting of SMC to design the adaptive laws	Consisting of the Wavelet membership function	Consisting of adaptive weights	Consisting of a Lyapunov function
8	TSKFCMAC [34]	Comprising a TSK fuzzy rule, a CMAC and it can be acted as a main controller	Consisting of SMC to design the adaptive laws	Consisting of the Gaussian membership function	Consisting of adaptive weights	Consisting of a Lyapunov function

calculated as

$$\begin{cases} e_1 = y_1 - x_1 \\ e_2 = y_2 - x_2 \\ e_3 = y_3 - x_3 \\ e_4 = y_4 - x_4 \\ e_5 = y_5 - x_5 \end{cases} \tag{3}$$

The error dynamics can be given by

$$\begin{cases} \dot{e}_1 = \dot{y}_1 - \dot{x}_1 = a_1 e_2 + a_2 e_4 + \Delta Y(y_1) + n_{d1} + u_1 \\ \dot{e}_2 = \dot{y}_2 - \dot{x}_2 = -a_1 e_1 - a_2 y_1 y_4 + a_2 x_1 x_4 \\ \qquad + \Delta Y(y_2) + n_{d2} + u_2 \\ \dot{e}_3 = \dot{y}_3 - \dot{x}_3 = a_3 e_4 + \Delta Y(y_3) + n_{d3} + u_3 \\ \dot{e}_4 = \dot{y}_4 - \dot{x}_4 = -a_4 e_3 - a_2 y_1 y_2 + a_2 x_1 x_2 \\ \qquad + \Delta Y(y_4) + n_{d4} + u_4 \\ \dot{e}_5 = \dot{y}_5 - \dot{x}_5 = -a_3 e_1 + \Delta Y(y_5) + n_{d5} + u_5 \end{cases} \tag{4}$$

Equation (4) can be presented by the vector form as

$$\dot{\boldsymbol{e}} = \mathrm{T}\boldsymbol{e} + \boldsymbol{\varphi} + \Delta Y(\boldsymbol{y}_S) + \boldsymbol{n}_d + \boldsymbol{u} \tag{5}$$

where

$$\boldsymbol{e} = [e_1, e_2, e_3, e_4, e_5]^T,$$

$$\mathrm{T} = \begin{bmatrix} 0 & a_1 & 0 & a_2 & 0 \\ -a_1 & 0 & 0 & 0 & 0 \\ 0 & 0 & 0 & a_3 & 0 \\ 0 & 0 & -a_4 & 0 & 0 \\ -a_3 & 0 & 0 & 0 & 0 \end{bmatrix},$$

and

$$\boldsymbol{\varphi} = \begin{bmatrix} 0 \\ -a_2 y_1 y_4 + a_2 x_1 x_4 \\ 0 \\ -a_2 y_1 y_2 + a_2 x_1 x_2 \\ 0 \end{bmatrix}$$

If $\Delta \boldsymbol{Y}(\boldsymbol{y})$ and $\boldsymbol{n}_d$ are known, an ideal control value can be defined as

$$\boldsymbol{u}^* = -\mathrm{T}\boldsymbol{e} - \boldsymbol{\varphi} - \Delta Y(\boldsymbol{y}_S) - \boldsymbol{n}_d - \boldsymbol{\Psi}\boldsymbol{e} \tag{6}$$

where $\boldsymbol{\Psi} = \mathrm{diag}(\psi_1, \psi_2, \psi_3, \psi_4, \psi_5)$ is the feedback gain matrix. Inserting (6) into (5) attains:

$$\dot{\boldsymbol{e}} + \boldsymbol{\Psi}\boldsymbol{e} = 0 \tag{7}$$

If $\boldsymbol{\Psi}$ can be regulated to fascinate the Hurwitz stability criterion, then $\lim_{t\to\infty} \boldsymbol{e} \to 0$. In fact, the ideal controller in (7) is not obtained because the lumped uncertainty, $\boldsymbol{n}_d(t)$, is not known for practical applications. Therefore, a wavelet-interval type-2 TSK fuzzy brain emotional learning cerebellar model articulation controller (WIT2TFBCC) is investigated to mimic the ideal controller. In this section, the proposed wavelet interval type-2 TSK fuzzy brain emotional learning cerebellar model articulation controller (WIT2TFBCC) is presented. The proposed structure includes two channels: The Wavelet Interval Type-2 TSK Cerebellar Model Articulation Controller channel (WIT2TFCMAC) and the Wavelet Interval Type-2 TSK Fuzzy Brain Emotional Learning Controller channel (WIT2TFBELC). The WIT2TFBELC channel contains four domains called *input domain*, *association memory domain*, *output weight domain*, and *sub-output domain*. The WIT2TFCMAC channel has five domains, besides four domains as similar as the WIT2TFBELC, it has one more domain called *receptive-field domain* which is located between the *associative memory domain* and *the weight memory domain*. The structure of the proposed algorithm is described in Fig 1.

A. THE INPUT DOMAIN

In this domain, the input variables are denoted by a vector $\boldsymbol{x} = \left[x_1, x_2, \ldots, x_i, \ldots, x_{n_i}\right]^T \in R^{n_i}$, where x_i and n_i are the i^{th} input variable and the input dimension, respectively.

B. WIT2TFBELC CHANNEL

1) ASSOCIATIVE MEMORY DOMAIN

This domain uses the wavelet interval type-2 membership function (WIT2MF).

$$\underline{a}_{iq} = \left(\frac{x_i - m_{iq}^B}{\underline{d}_{iq}^B}\right) \exp\left(-\frac{\left(x_i - m_{iq}^B\right)^2}{2\underline{d}_{iq}^{B^2}}\right) \tag{8}$$

and

$$\overline{a}_{iq} = \left(\frac{x_i - m_{iq}^B}{\overline{d}_{iq}^B}\right) \exp\left(-\frac{\left(x_i - m_{iq}^B\right)^2}{2\overline{d}_{iq}^{B^2}}\right) \tag{9}$$

where m_{iq}^B, $\underline{d}_q^B$ and $\overline{d}_{iq}^B$ are respectively the center, the lower variance and the upper variance of the WIT2MF.

$$\begin{cases} \overline{a}_q = \sum_{i=1}^{n_i} \overline{a}_{iq} \\ \underline{a}_q = \sum_{i=1}^{n_i} \underline{a}_{iq} \end{cases} \tag{10}$$

Set

$$\begin{cases} \overline{\boldsymbol{a}} = \left[\overline{a}_1, \ldots, \overline{a}_q, \ldots, \overline{a}_{n_q}\right]^T \in \Re^{n_q} \\ \underline{\boldsymbol{a}} = \left[\underline{a}_1, \ldots, \underline{a}_q, \ldots, \overline{a}_{n_q}\right]^T \in \Re^{n_q} \end{cases} \tag{11}$$

2) WEIGHT MEMORY DOMAIN

In this research, the weight is formed by the TSK fuzzy inference system. The following reference rules are exploited:

$$R^q: \text{ If } x_1 \text{ is } a_{1q}, x_2 \text{ is } a_{2q}, \ldots, \text{ and } a_{n_i} \text{ is } a_{n_i q},$$

then

$$w_q^B = x_1 t_{1q}^B + x_2 t_{2q}^B \ldots + x_{n_i} t_{n_i q}^B \tag{12}$$

for $i = 1, 2, \cdots, n_i$, where q is the number of fuzzy rules, $q = 1, 2, \ldots, n_q$ in which n_q is the fuzzy rules dimension, and a_{iq} is the fuzzy set for the i- th input, q- th output; and w_q^B is the TSK-type output weight of WIT2TFBELC. Defining the weight matrix for WIT2TFBELC channel

$$\begin{aligned} \overline{\boldsymbol{w}}^B &= \begin{bmatrix} \overline{w}_1^B \\ \vdots \\ \overline{w}_q^B \\ \vdots \\ \overline{w}_{n_q}^B \end{bmatrix} = \begin{bmatrix} \overline{t}_{11}^B & \ldots & \overline{t}_{i1}^B & \ldots & \overline{t}_{n_i 1}^B \\ \vdots & \ldots & \vdots & \ldots & \vdots \\ \overline{t}_{1q}^B & \ldots & \overline{t}_{iq}^B & \ldots & \overline{t}_{n_i q}^B \\ \vdots & \ldots & \vdots & \ldots & \vdots \\ \overline{t}_{1n_q}^B & \ldots & \overline{t}_{in_q}^B & \ldots & \overline{t}_{n_i n_q}^B \end{bmatrix} \begin{bmatrix} x_1 \\ \vdots \\ x_i \\ \vdots \\ x_{n_i} \end{bmatrix} = \overline{\boldsymbol{t}}^{B^T} \boldsymbol{x} \\ \underline{\boldsymbol{w}}^B &= \begin{bmatrix} \underline{w}_1^B \\ \vdots \\ \underline{w}_q^B \\ \vdots \\ \underline{w}_{n_q}^B \end{bmatrix} = \begin{bmatrix} \underline{t}_{11}^B & \ldots & \underline{t}_{i1}^B & \ldots & \underline{t}_{n_i 1}^B \\ \vdots & \ldots & \vdots & \ldots & \vdots \\ \underline{t}_{1q}^B & \ldots & \underline{t}_{iq}^B & \ldots & \underline{t}_{n_i q}^B \\ \vdots & \ldots & \vdots & \ldots & \vdots \\ \underline{t}_{1n_q}^B & \ldots & \underline{t}_{in_q}^B & \ldots & \underline{t}_{n_i n_q}^B \end{bmatrix} \begin{bmatrix} x_1 \\ \vdots \\ x_i \\ \vdots \\ x_{n_i} \end{bmatrix} = \underline{\boldsymbol{t}}^{B^T} \boldsymbol{x} \end{aligned} \tag{13}$$

where

$$\overline{\boldsymbol{t}}^{B^T} = \begin{bmatrix} \overline{\boldsymbol{t}}_{11}^B \\ \vdots \\ \overline{\boldsymbol{t}}_{jk}^B \\ \vdots \\ \overline{\boldsymbol{t}}_{n_j n_k}^B \end{bmatrix} = \begin{bmatrix} \overline{t}_{11}^B & \ldots & \overline{t}_{i1}^B & \ldots & \overline{t}_{n_i 1}^B \\ \vdots & \ldots & \vdots & \ldots & \vdots \\ \overline{t}_{1q}^B & \ldots & \overline{t}_{iq}^B & \ldots & \overline{t}_{n_i q}^B \\ \vdots & \ldots & \vdots & \ldots & \vdots \\ \overline{t}_{1n_q}^B & \ldots & \overline{t}_{in_q}^B & \ldots & \overline{t}_{n_i n_q}^B \end{bmatrix} \in \Re^{n_i \times n_q}$$

and

$$\underline{\boldsymbol{t}}^{B^T} = \begin{bmatrix} \underline{\boldsymbol{t}}_{11}^B \\ \vdots \\ \underline{\boldsymbol{t}}_{jk}^B \\ \vdots \\ \underline{\boldsymbol{t}}_{n_j n_k}^B \end{bmatrix} = \begin{bmatrix} \underline{t}_{11}^B & \ldots & \underline{t}_{i1}^B & \ldots & \underline{t}_{n_i 1}^B \\ \vdots & \ldots & \vdots & \ldots & \vdots \\ \underline{t}_{1q}^B & \ldots & \underline{t}_{iq}^B & \ldots & \underline{t}_{n_i q}^B \\ \vdots & \ldots & \vdots & \ldots & \vdots \\ \underline{t}_{1n_q}^B & \ldots & \underline{t}_{in_q}^B & \ldots & \underline{t}_{n_i n_q}^B \end{bmatrix} \in \Re^{n_i \times n_q}$$

3) SUB-OUTPUT DOMAIN

$$a_q^l = \frac{\sum_{q=1}^{n_q} a_q^l w_q^B}{\sum_{q=1}^{n_q} a_q^l} = \frac{\sum_{q=1}^{n_q} a_q^l \underline{\boldsymbol{t}}_q^{B^T} \boldsymbol{x}}{\sum_{q=1}^{n_q} a_q^l} \tag{14}$$

$$a_q^r = \frac{\sum_{q=1}^{n_q} a_q^r \overline{w}_q^B}{\sum_{q=1}^{n_q} a_q^r} = \frac{\sum_{q=1}^{n_q} a_q^r \overline{\boldsymbol{t}}_q^{B^T} \boldsymbol{x}}{\sum_{q=1}^{n_q} a_q^r} \tag{15}$$

where a_{jk}^l and a_{jk}^r are determined by Karnik-Mendel algorithm [28]

$$a_q^l = \begin{cases} \overline{a}_q, & q \le \mathrm{L_s} \\ \underline{a}_q, & q > \mathrm{L_s} \end{cases} \tag{16}$$

and

$$a_q^r = \begin{cases} \underline{a}_q, & q \le \mathrm{R_s} \\ \overline{a}_q, & q > \mathrm{R_s} \end{cases} \tag{17}$$

where and $\mathrm{L_s}$ and $\mathrm{R_s}$ are the left and right switch points, then

$$a_q = \frac{a_q^l + a_q^r}{2} \tag{18}$$

C. WIT2TFCMAC CHANNEL

1) ASSOCIATIVE MEMORY DOMAIN

$$\underline{o}_{iq} = \left(\frac{x_i - m_{iq}^C}{\underline{d}_{iq}^C}\right) \exp\left(-\frac{\left(x_i - m_{iq}^C\right)^2}{2\underline{d}_{iq}^{C^2}}\right) \tag{19}$$

$$\overline{o}_{iq} = \left(\frac{x_i - m_{iq}^C}{\overline{d}_{iq}^C}\right) \exp\left(-\frac{\left(x_i - m_{iq}^C\right)^2}{2\overline{d}_{iq}^{C^2}}\right) \tag{20}$$

where m_{iq}^C, $\underline{d}_{iq}^C$ and $\overline{d}_{iq}^C$ are the center, the lower variance and the upper variance of the WIT2MF, respectively.

2) RECEPTIVE-FIELD DOMAIN

Each block value is the product of the equivalent block of the associative memory domain, which is determined by:

$$\begin{cases} \underline{o}_q = \prod_{i=1}^{n_i} \underline{o}_{iq} \\ \overline{o}_q = \prod_{i=1}^{n_i} \overline{o}_{iq} \end{cases} \tag{21}$$

Set

$$\overline{\boldsymbol{o}} = \left[\overline{o}_1, \ldots, \overline{o}_q, \ldots, \overline{o}_{n_q}\right]^T \in \Re^{n_q} \tag{22}$$

and

$$\underline{\boldsymbol{o}} = \left[\underline{o}_1, \ldots, \underline{o}_q, \ldots, \underline{o}_{n_q}\right]^T \in \Re^{n_q} \tag{23}$$

3) WEIGHT MEMORY DOMAIN

Define the weight matrix for the CMAC channel with TSK fuzzy reasoning as follows

$$\begin{aligned} &R^q: \text{ If } x_1 \text{ is } o_{1q}, x_2 \text{ is } o_{2q}, \ldots, \text{ and } o_{n_i} \text{ is } o_{n_i q}, \\ &\text{then } w_q^C = x_1 t_{1q}^C + x_2 t_{2q}^C \ldots + x_{n_i} t_{n_i q}^C \\ &\text{for } i = 1, 2, \cdots, n_i \end{aligned} \tag{24}$$

where w_q^C is the TSK-type output weight of TSKCMAC. For detail, using the wavelet interval type-2 function, the weight matrix is defined as follows:

$$\begin{aligned} \overline{\boldsymbol{w}}^C &= \begin{bmatrix} \overline{\boldsymbol{w}}_1^C \\ \vdots \\ \overline{\boldsymbol{w}}_q^C \\ \vdots \\ \overline{\boldsymbol{w}}_{n_q}^C \end{bmatrix} = \begin{bmatrix} \overline{t}_{11}^C & \cdots & \overline{t}_{i1}^C & \cdots & \overline{t}_{n_i 1}^C \\ \vdots & \cdots & \vdots & \cdots & \vdots \\ \overline{t}_{1q}^C & \cdots & \overline{t}_{iq}^C & \cdots & \overline{t}_{n_i q}^C \\ \vdots & \cdots & \vdots & \cdots & \vdots \\ \overline{t}_{1n_q}^C & \cdots & \overline{t}_{in_q}^C & \cdots & \overline{t}_{n_i n_q}^C \end{bmatrix} \cdot \begin{bmatrix} x_1 \\ \vdots \\ x_i \\ \vdots \\ x_{n_i} \end{bmatrix} \\ &= \overline{\boldsymbol{t}}^{C^T} \boldsymbol{.x} \\ \underline{\boldsymbol{w}}^C &= \begin{bmatrix} \underline{\boldsymbol{w}}_1^C \\ \vdots \\ \underline{\boldsymbol{w}}_q^C \\ \vdots \\ \underline{\boldsymbol{w}}_{n_q}^C \end{bmatrix} = \begin{bmatrix} \underline{t}_{11}^C & \cdots & \underline{t}_{i1}^C & \cdots & \underline{t}_{n_i 1}^C \\ \vdots & \cdots & \vdots & \cdots & \vdots \\ \underline{t}_{1q}^C & \cdots & \underline{t}_{iq}^C & \cdots & \underline{t}_{n_i q}^C \\ \vdots & \cdots & \vdots & \cdots & \vdots \\ \underline{t}_{1n_q}^C & \cdots & \underline{t}_{in_q}^C & \cdots & \underline{t}_{n_i n_q}^C \end{bmatrix} \cdot \begin{bmatrix} x_1 \\ \vdots \\ x_i \\ \vdots \\ x_{n_i} \end{bmatrix} \\ &= \underline{\boldsymbol{t}}^{C^T} \boldsymbol{.x} \end{aligned} \tag{25}$$

where

$$\overline{\boldsymbol{t}}^{C^T} = \begin{bmatrix} \overline{\boldsymbol{t}}_1^C \\ \vdots \\ \overline{\boldsymbol{t}}_q^C \\ \vdots \\ \overline{\boldsymbol{t}}_{n_q}^C \end{bmatrix} = \begin{bmatrix} \overline{t}_{11}^C & \cdots & \overline{t}_{i1}^C & \cdots & \overline{t}_{n_i 1}^C \\ \vdots & \cdots & \vdots & \cdots & \vdots \\ \overline{t}_{1q}^C & \cdots & \overline{t}_{iq}^C & \cdots & \overline{t}_{n_i q}^C \\ \vdots & \cdots & \vdots & \cdots & \vdots \\ \overline{t}_{1n_q}^C & \cdots & \overline{t}_{in_q}^C & \cdots & \overline{t}_{n_i n_q}^C \end{bmatrix} \in \Re^{n_i \times n_q}$$

$$\underline{\boldsymbol{t}}^{C^T} = \begin{bmatrix} \underline{\boldsymbol{t}}_1^C \\ \vdots \\ \underline{\boldsymbol{t}}_q^C \\ \vdots \\ \underline{\boldsymbol{t}}_{n_q}^C \end{bmatrix} = \begin{bmatrix} \underline{t}_{11}^C & \cdots & \underline{t}_{i1}^C & \cdots & \underline{t}_{n_i 1}^C \\ \vdots & \cdots & \vdots & \cdots & \vdots \\ \underline{t}_{1q}^C & \cdots & \underline{t}_{iq}^C & \cdots & \underline{t}_{n_i q}^C \\ \vdots & \cdots & \vdots & \cdots & \vdots \\ \underline{t}_{1n_q}^C & \cdots & \underline{t}_{in_q}^C & \cdots & \underline{t}_{n_i n_q}^C \end{bmatrix} \in \Re^{n_i \times n_q}$$

4) SUB-OUTPUT DOMAIN

The q-th output of the network is determined by the weight memory domain and the Associative memory domain.

$$o_q^l = \frac{\sum_{q=1}^{n_q} o_q^l \underline{w}_q^C}{\sum_{q=1}^{n_q} o_q^l} = \frac{\sum_{q=1}^{n_q} o_q^l \underline{\boldsymbol{t}}_q^{C^T} \boldsymbol{x}}{\sum_{q=1}^{n_q} o_q^l} \tag{26}$$

$$o_q^r = \frac{\sum_{q=1}^{n_q} o_q^r \overline{w}_q^C}{\sum_{q=1}^{n_q} o_q^r} = \frac{\sum_{q=1}^{n_q} o_q^r \overline{\boldsymbol{t}}_q^{C^T} \boldsymbol{x}}{\sum_{q=1}^{n_q} o_q^r} \tag{27}$$

where o_q^l and o_q^r are determined by Karnik-Mendel algorithm [28], and $\mathrm{L_s}$ and $\mathrm{R_s}$ are the left and right switch points:

$$o_q^l = \begin{cases} \overline{o}_q, & q \le \mathrm{L_s} \\ \underline{o}_q, & q > \mathrm{L_s} \end{cases} \tag{28}$$

$$o_q^r = \begin{cases} \underline{o}_q, & q \le \mathrm{R_s} \\ \overline{o}_q, & q > \mathrm{R_s} \end{cases} \tag{29}$$

then

$$o_q = \frac{o_q^l + o_q^r}{2} \tag{30}$$

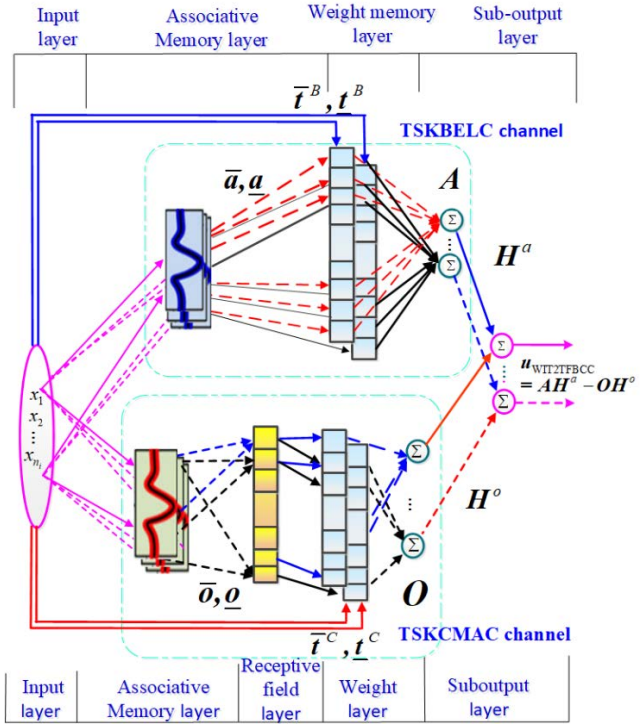

FIGURE 1. The structure of proposed WIT2TFBCC controller.

D. THE OUTPUT DOMAIN

Set

$$\boldsymbol{A}=\left[a_1,\ldots,a_q,\ldots,a_{n_q}\right],\quad \boldsymbol{O}=\left[o_1,\ldots,o_q,\ldots,o_{n_q}\right],$$
$$\boldsymbol{H}^a=\left[h_1^a,\ldots,h_q^a,\ldots,h_{n_q}^a\right]^T,$$
$$\boldsymbol{H}^o=\left[h_1^o,\ldots,h_q^o,\ldots,h_{n_q}^o\right]^T$$

Fig. 1 illustrates the proposed WIT2TFBCC. The controller output is defined as:

$$\boldsymbol{u}_{\mathrm{WIT2TFBCC}}=\boldsymbol{A}\boldsymbol{H}^a-\boldsymbol{O}\boldsymbol{H}^o \tag{31}$$

E. CONVERGENCE ANALYSIS

In practice there is always an error between the ideal controller and the WIT2TFBCC controller

$$\boldsymbol{u}=\hat{\boldsymbol{u}}_{\mathrm{WIT2TFBCC}}+\boldsymbol{\varepsilon}=\hat{\boldsymbol{A}}\hat{\boldsymbol{H}}^a-\hat{\boldsymbol{O}}\hat{\boldsymbol{H}}^o+\boldsymbol{\varepsilon} \tag{32}$$

where $\hat{\boldsymbol{A}},\hat{\boldsymbol{H}}^a,\hat{\boldsymbol{O}}$, and $\hat{\boldsymbol{H}}^o$ are respectively the estimated values of $\boldsymbol{A},\boldsymbol{H}^a,\boldsymbol{O}$, and $\boldsymbol{H}^o$.

$\boldsymbol{\varepsilon}$ is the minimum error between $\boldsymbol{u}^*$ and $\boldsymbol{u}_{\mathrm{WIT2TFBCC}}$(for $0\le\boldsymbol{\varepsilon}\le\boldsymbol{\kappa}$, where $\boldsymbol{\kappa}$ is constant vector), $\boldsymbol{A}^*$ and $\boldsymbol{O}^*$ are optimal parameters for $\boldsymbol{A}$ and $\boldsymbol{O}$, respectively. But $\boldsymbol{u}^*_{\mathrm{WIT2TFBCC}}$ can be unattained, therefore an online estimation of the WIT2TFBCC, $\boldsymbol{u}_{\mathrm{WIT2TFBCC}}$, is applied to estimate $\boldsymbol{u}_{\mathrm{WIT2TFBCC}}$. Using (25), equation (26) becomes

$$\boldsymbol{u}=\boldsymbol{u}_{\mathrm{WIT2TBCC}}+\boldsymbol{u}_{\mathrm{rb}}=\hat{\boldsymbol{A}}\hat{\boldsymbol{H}}^a-\hat{\boldsymbol{O}}\hat{\boldsymbol{H}}^o+\boldsymbol{u}_{\mathrm{rb}} \tag{33}$$

where $\boldsymbol{u}_{\mathrm{rb}}$ is a robust controller which rejects the approximate error $\boldsymbol{\varepsilon}$. The estimation error, $\tilde{\boldsymbol{u}}$, is calculated by subtracting (33) from (32) as follows:

$$\begin{aligned}\tilde{\boldsymbol{u}}&=\boldsymbol{u}^*-\boldsymbol{u}=\boldsymbol{A}^*\boldsymbol{H}^{*a}-\boldsymbol{O}^*\boldsymbol{H}^{*o}-(\hat{\boldsymbol{A}}\hat{\boldsymbol{H}}^a-\hat{\boldsymbol{O}}\hat{\boldsymbol{H}}^o)+\boldsymbol{\varepsilon}-\boldsymbol{u}_{\mathrm{rb}}\\&=\hat{\boldsymbol{A}}\tilde{\boldsymbol{H}}^a+\tilde{\boldsymbol{A}}\hat{\boldsymbol{H}}^a+\tilde{\boldsymbol{A}}\tilde{\boldsymbol{H}}^a-(\hat{\boldsymbol{O}}\tilde{\boldsymbol{H}}^o+\hat{\boldsymbol{O}}\hat{\boldsymbol{H}}^o+\tilde{\boldsymbol{O}}\tilde{\boldsymbol{H}}^o)+\boldsymbol{\varepsilon}-\boldsymbol{u}_{\mathrm{rb}}\\&=\hat{\boldsymbol{A}}\tilde{\boldsymbol{H}}^a+\tilde{\boldsymbol{A}}\hat{\boldsymbol{H}}^a+\tilde{\boldsymbol{A}}\tilde{\boldsymbol{H}}^a-\hat{\boldsymbol{O}}\tilde{\boldsymbol{H}}^o-\hat{\boldsymbol{O}}\hat{\boldsymbol{H}}^o-\tilde{\boldsymbol{O}}\tilde{\boldsymbol{H}}^o+\boldsymbol{\varepsilon}-\boldsymbol{u}_{\mathrm{rb}}\\&=\hat{\boldsymbol{A}}\tilde{\boldsymbol{H}}^a+\tilde{\boldsymbol{A}}\hat{\boldsymbol{H}}^a-\hat{\boldsymbol{O}}\tilde{\boldsymbol{H}}^o-\tilde{\boldsymbol{O}}\hat{\boldsymbol{H}}^o+\tilde{\boldsymbol{A}}\tilde{\boldsymbol{H}}^a-\tilde{\boldsymbol{O}}\tilde{\boldsymbol{H}}^o+\boldsymbol{\varepsilon}-\boldsymbol{u}_{\mathrm{rb}}\end{aligned} \tag{34}$$

where $\tilde{\boldsymbol{A}}=\boldsymbol{A}^*-\hat{\boldsymbol{A}},\tilde{\boldsymbol{O}}=\boldsymbol{O}^*-\hat{\boldsymbol{O}}$. The expansion of $\tilde{\boldsymbol{A}}$ and $\tilde{\boldsymbol{O}}$ in the Taylor series can be achieved as [11]:

$$\begin{cases}\tilde{\boldsymbol{A}}=\boldsymbol{A}_m\tilde{\boldsymbol{m}}^B+\boldsymbol{A}_{\underline{\boldsymbol{d}}^B}\tilde{\underline{\boldsymbol{d}}}^B+\boldsymbol{A}_{\overline{\boldsymbol{d}}^B}\tilde{\overline{\boldsymbol{d}}}^B+\boldsymbol{A}_{\underline{\boldsymbol{t}}^B}\tilde{\underline{\boldsymbol{t}}}^B+\boldsymbol{A}_{\overline{\boldsymbol{t}}^B}\tilde{\overline{\boldsymbol{t}}}^B+\boldsymbol{T}_a\\ \tilde{\boldsymbol{O}}=\boldsymbol{O}_m\tilde{\boldsymbol{m}}^C+\boldsymbol{O}_{\underline{\boldsymbol{d}}^C}\tilde{\underline{\boldsymbol{d}}}^C+\boldsymbol{O}_{\overline{\boldsymbol{d}}^C}\tilde{\overline{\boldsymbol{d}}}^C+\boldsymbol{O}_{\underline{\boldsymbol{t}}^C}\tilde{\underline{\boldsymbol{t}}}^C+\boldsymbol{O}_{\overline{\boldsymbol{t}}^C}\tilde{\overline{\boldsymbol{t}}}^C+\boldsymbol{T}_o\end{cases} \tag{35}$$

where $\tilde{\boldsymbol{m}}^B=\boldsymbol{m}^{B*}-\hat{\boldsymbol{m}}^B,\tilde{\boldsymbol{m}}^C=\boldsymbol{m}^{C*}-\hat{\boldsymbol{m}}^C,\tilde{\underline{\boldsymbol{d}}}^B=\underline{\boldsymbol{d}}^{B*}-\hat{\underline{\boldsymbol{d}}}^B,\tilde{\underline{\boldsymbol{d}}}^C=\underline{\boldsymbol{d}}^{C*}-\hat{\underline{\boldsymbol{d}}}^C,\tilde{\overline{\boldsymbol{d}}}^B=\overline{\boldsymbol{d}}^{B*}-\hat{\overline{\boldsymbol{d}}}^B,\tilde{\overline{\boldsymbol{d}}}^C=\overline{\boldsymbol{d}}^{C*}-\hat{\overline{\boldsymbol{d}}}^C,\tilde{\underline{\boldsymbol{t}}}^B=\underline{\boldsymbol{t}}^{B*}-\hat{\underline{\boldsymbol{t}}},\tilde{\overline{\boldsymbol{t}}}^B=\overline{\boldsymbol{t}}^{B*}-\hat{\overline{\boldsymbol{t}}}^B,\tilde{\underline{\boldsymbol{t}}}^C=\underline{\boldsymbol{t}}^{C*}-\hat{\underline{\boldsymbol{t}}}^C,\tilde{\overline{\boldsymbol{t}}}^C=\overline{\boldsymbol{t}}^{C*}-\hat{\overline{\boldsymbol{t}}}^C$; $\boldsymbol{T}_A$ and $\boldsymbol{T}_O$ are respectively higher-order term vectors of $\boldsymbol{A}$, O; $\frac{\partial a_q}{\partial \boldsymbol{m}^B}$, $\frac{\partial o_q}{\partial \boldsymbol{m}^C}$, $\frac{\partial A}{\partial \underline{\boldsymbol{d}}^B}$, $\frac{\partial O}{\partial \underline{\boldsymbol{d}}^C}$, $\frac{\partial \boldsymbol{A}}{\partial \overline{\boldsymbol{d}}^B}$, $\frac{\partial O}{\partial \overline{\boldsymbol{d}}^C}$, $\frac{\partial \boldsymbol{A}}{\partial \underline{\boldsymbol{t}}^B}$, $\frac{\partial \boldsymbol{A}}{\partial \overline{\boldsymbol{t}}^B}$, $\frac{\partial \mathrm{O}}{\partial \underline{\boldsymbol{t}}^C}$, $\frac{\partial \mathrm{O}}{\partial \overline{\boldsymbol{t}}^B}$ are defined by:

$$\left[\frac{\partial a_q}{\partial \boldsymbol{m}^B}\right]=\left[\underbrace{0,\cdots,0}_{(q-1)\times n_i},\frac{\partial a_q}{\partial m^B_{1q}},\ldots,\frac{\partial A_{n_q}}{\partial m^B_{n_iq}},\underbrace{0,\cdots,0}_{(n_q-q)\times n_i}\right] \tag{36}$$

$$\left[\frac{\partial a_q}{\partial \underline{\boldsymbol{d}}^B}\right]=\left[\underbrace{0,\cdots,0}_{(q-1)\times n_i},\frac{\partial a_q}{\partial \underline{d}^B_{1q}},\ldots,\frac{\partial a_q}{\partial \underline{d}^B_{n_iq}},\underbrace{0,\cdots,0}_{(n_q-q)\times n_i}\right] \tag{37}$$

$$\left[\frac{\partial a_q}{\partial \overline{\boldsymbol{d}}^B}\right]=\left[\underbrace{0,\cdots,0}_{(q-1)\times n_i},\frac{\partial a_q}{\partial \overline{d}^B_{1q}},\ldots,\frac{\partial a_q}{\partial \overline{d}^B_{n_iq}},\underbrace{0,\cdots,0}_{(n_q-q)\times n_i}\right] \tag{38}$$

$$\left[\frac{\partial a_q}{\partial \underline{\boldsymbol{t}}^B}\right]=\left[\underbrace{0,\cdots,0}_{(q-1)\times n_i},\frac{\partial a_q}{\partial \underline{t}^B_{1q}},\ldots,\frac{\partial a_q}{\partial \underline{t}^B_{n_iq}},\underbrace{0,\cdots,0}_{(n_q-q)\times n_i}\right] \tag{39}$$

$$\left[\frac{\partial a_q}{\partial \overline{\boldsymbol{t}}^B}\right]=\left[\underbrace{0,\cdots,0}_{(q-1)\times n_i},\frac{\partial a_q}{\partial \overline{t}^B_{1q}},\ldots,\frac{\partial a_q}{\partial \overline{t}^B_{n_iq}},\underbrace{0,\cdots,0}_{(n_q-q)\times n_i}\right] \tag{40}$$

$$\left[\frac{\partial o_q}{\partial \boldsymbol{m}^C}\right]=\left[\underbrace{0,\cdots,0}_{(q-1)\times n_i},\frac{\partial o_q}{\partial m^C_{1q}},\ldots,\frac{\partial o_q}{\partial m^C_{n_iq}},\underbrace{0,\cdots,0}_{(n_q-q)\times n_i}\right] \tag{41}$$

$$\left[\frac{\partial o_q}{\partial \underline{\boldsymbol{d}}^C}\right]=\left[\underbrace{0,\cdots,0}_{(q-1)\times n_i},\frac{\partial o_q}{\partial \underline{d}^C_{1q}},\ldots,\frac{\partial o_q}{\partial \underline{d}^C_{n_iq}},\underbrace{0,\cdots,0}_{(n_q-q)\times n_i}\right] \tag{42}$$

$$\left[\frac{\partial o_q}{\partial \overline{\boldsymbol{d}}^C}\right]=\left[\underbrace{0,\cdots,0}_{(q-1)\times n_i},\frac{\partial o_q}{\partial \overline{d}^C_{1q}},\ldots,\frac{\partial o_q}{\partial \overline{d}^C_{n_iq}},\underbrace{0,\cdots,0}_{(n_q-q)\times n_i}\right] \tag{43}$$

$$\left[\frac{\partial o_q}{\partial \underline{t}^C}\right] = \left[\underbrace{0,\cdots,0}_{(q-1)\times n_i}, \frac{\partial o_q}{\partial \underline{t}_{1q}^C},\ldots,\frac{\partial o_q}{\partial \underline{t}_{n_i q}^C}, \underbrace{0,\cdots,0}_{(n_q-q)\times n_i}\right] \tag{44}$$

$$\left[\frac{\partial o_q}{\partial \bar{t}^C}\right] = \left[\underbrace{0,\cdots,0}_{(q-1)\times n_i}, \frac{\partial o_q}{\partial \bar{t}_{1q}^C},\ldots,\frac{\partial o_q}{\partial \bar{t}_{n_i q}^C}, \underbrace{0,\cdots,0}_{(n_q-q)\times n_i}\right] \tag{45}$$

Inserting (35) into (34) obtains

$$\begin{aligned}\tilde{\boldsymbol{u}} &= \hat{\boldsymbol{A}}\tilde{\boldsymbol{H}}^a + (\boldsymbol{A}_{\boldsymbol{m}^B}\tilde{\boldsymbol{m}}^B + \boldsymbol{A}_{\underline{\boldsymbol{d}}^B}\tilde{\underline{\boldsymbol{d}}}^B + \boldsymbol{A}_{\bar{\boldsymbol{d}}^B}\tilde{\bar{\boldsymbol{d}}}^B + \boldsymbol{A}_{\underline{\boldsymbol{t}}^B}\tilde{\underline{\boldsymbol{t}}}^B + \boldsymbol{A}_{\bar{\boldsymbol{t}}^B}\tilde{\bar{\boldsymbol{t}}}^B + \boldsymbol{T}_a) \\ &\quad \times \hat{\boldsymbol{H}}^a - \hat{\boldsymbol{O}}\tilde{\boldsymbol{H}}^o - (\boldsymbol{O}_{\boldsymbol{m}^C}\tilde{\boldsymbol{m}}^C + \boldsymbol{O}_{\underline{\boldsymbol{d}}^C}\tilde{\underline{\boldsymbol{d}}}^C + \boldsymbol{O}_{\bar{\boldsymbol{d}}^C}\tilde{\bar{\boldsymbol{d}}}^C + \boldsymbol{O}_{\underline{\boldsymbol{t}}^C}\tilde{\underline{\boldsymbol{t}}}^C \\ &\quad + \boldsymbol{O}_{\bar{\boldsymbol{t}}^C}\tilde{\bar{\boldsymbol{t}}}^C + \boldsymbol{T}_o)\hat{\boldsymbol{H}}^o + \tilde{\boldsymbol{A}}\tilde{\boldsymbol{H}}^a - \tilde{\boldsymbol{O}}\tilde{\boldsymbol{H}}^o + \boldsymbol{\varepsilon} - \boldsymbol{u}_{\text{rb}} \\ &= \hat{\boldsymbol{A}}\tilde{\boldsymbol{H}}^a - \hat{\boldsymbol{O}}\tilde{\boldsymbol{H}}^o + \boldsymbol{A}_{\boldsymbol{m}^B}\tilde{\boldsymbol{m}}^B\hat{\boldsymbol{H}}^a + \boldsymbol{A}_{\underline{\boldsymbol{d}}^B}\tilde{\underline{\boldsymbol{d}}}^B\hat{\boldsymbol{H}}^a + \boldsymbol{A}_{\bar{\boldsymbol{d}}^B}\tilde{\bar{\boldsymbol{d}}}^B\hat{\boldsymbol{H}}^a \\ &\quad + \boldsymbol{A}_{\underline{\boldsymbol{t}}^B}\tilde{\underline{\boldsymbol{t}}}^B\hat{\boldsymbol{H}}^a + \boldsymbol{A}_{\bar{\boldsymbol{t}}^B}\tilde{\bar{\boldsymbol{t}}}^B\hat{\boldsymbol{H}}^a - (\boldsymbol{O}_{\boldsymbol{m}^C}\tilde{\boldsymbol{m}}^C\hat{\boldsymbol{H}}^o + \boldsymbol{O}_{\underline{\boldsymbol{d}}^C}\tilde{\underline{\boldsymbol{d}}}^C\hat{\boldsymbol{H}}^o \\ &\quad + \boldsymbol{O}_{\bar{\boldsymbol{d}}^C}\tilde{\bar{\boldsymbol{d}}}^C\hat{\boldsymbol{H}}^o + \boldsymbol{O}_{\underline{\boldsymbol{t}}^C}\tilde{\underline{\boldsymbol{t}}}^C\hat{\boldsymbol{H}}^o + \boldsymbol{O}_{\bar{\boldsymbol{t}}^C}\tilde{\bar{\boldsymbol{t}}}^C\hat{\boldsymbol{H}}^o)\boldsymbol{T}_a\hat{\boldsymbol{H}}^a - \boldsymbol{T}_o\hat{\boldsymbol{H}}^o \\ &\quad + \tilde{\boldsymbol{A}}\tilde{\boldsymbol{H}}^a - \tilde{\boldsymbol{O}}\tilde{\boldsymbol{H}}^o + \boldsymbol{\varepsilon} - \boldsymbol{u}_{\text{rb}} \\ &= \hat{\boldsymbol{A}}\tilde{\boldsymbol{H}}^a - \hat{\boldsymbol{O}}\tilde{\boldsymbol{H}}^o + \boldsymbol{A}_{\boldsymbol{m}^B}\tilde{\boldsymbol{m}}^B\hat{\boldsymbol{H}}^a + \boldsymbol{A}_{\underline{\boldsymbol{d}}^B}\tilde{\underline{\boldsymbol{d}}}^B\hat{\boldsymbol{H}}^a + \boldsymbol{A}_{\bar{\boldsymbol{d}}^B}\tilde{\bar{\boldsymbol{d}}}^B\hat{\boldsymbol{H}}^a \\ &\quad + \boldsymbol{A}_{\underline{\boldsymbol{t}}^B}\tilde{\underline{\boldsymbol{t}}}^B\hat{\boldsymbol{H}}^a + \boldsymbol{A}_{\bar{\boldsymbol{t}}^B}\tilde{\bar{\boldsymbol{t}}}^B\hat{\boldsymbol{H}}^a - \boldsymbol{O}_{\boldsymbol{m}^C}\tilde{\boldsymbol{m}}^C\hat{\boldsymbol{H}}^o - \boldsymbol{O}_{\underline{\boldsymbol{d}}^C}\tilde{\underline{\boldsymbol{d}}}^C\hat{\boldsymbol{H}}^o \\ &\quad - \boldsymbol{O}_{\bar{\boldsymbol{d}}^C}\tilde{\bar{\boldsymbol{d}}}^C\hat{\boldsymbol{H}}^o - \boldsymbol{O}_{\underline{\boldsymbol{t}}^B}\tilde{\underline{\boldsymbol{t}}}^C\hat{\boldsymbol{H}}^o - \boldsymbol{O}_{\bar{\boldsymbol{t}}^C}\tilde{\bar{\boldsymbol{t}}}^C\hat{\boldsymbol{H}}^o + \boldsymbol{\theta} - \boldsymbol{u}_{\text{rb}} \end{aligned} \tag{46}$$

where the cumulative error, $\boldsymbol{\theta} = \boldsymbol{T}_a\hat{\boldsymbol{H}}^a - \boldsymbol{T}_o\hat{\boldsymbol{H}}^o + \tilde{\boldsymbol{A}}\tilde{\boldsymbol{H}}^a - \tilde{\boldsymbol{O}}\tilde{\boldsymbol{H}}^o + \boldsymbol{\varepsilon}$ is assumed to be bounded by $\|\boldsymbol{\theta}\| < \boldsymbol{\kappa}$. Defining the sliding surface as $\boldsymbol{s} = \boldsymbol{e} + \boldsymbol{\Psi}\int_0^t \boldsymbol{e}(\tau)d\tau$. The derivate of $\boldsymbol{s}$ can be calculated by (6), (7), and (34) as follows

$$\begin{aligned}\dot{\boldsymbol{s}} &= \dot{\boldsymbol{e}} + \boldsymbol{\Psi}\boldsymbol{e} = \boldsymbol{u}^* - \boldsymbol{u} \\ &= \hat{\boldsymbol{A}}\tilde{\boldsymbol{H}}^a - \hat{\boldsymbol{O}}\tilde{\boldsymbol{H}}^o + \hat{\boldsymbol{H}}^{aT}\boldsymbol{A}_{\boldsymbol{m}^B}\tilde{\boldsymbol{m}}^B + \hat{\boldsymbol{H}}^{aT}\boldsymbol{A}_{\underline{\boldsymbol{d}}^B}\tilde{\underline{\boldsymbol{d}}}^B \\ &\quad + \hat{\boldsymbol{H}}^{aT}\boldsymbol{A}_{\bar{\boldsymbol{d}}^B}\tilde{\bar{\boldsymbol{d}}}^B - \hat{\boldsymbol{H}}^{oT}\boldsymbol{O}_{\boldsymbol{m}^C}\tilde{\boldsymbol{m}}^C - \hat{\boldsymbol{H}}^{oT}\boldsymbol{O}_{\underline{\boldsymbol{d}}^C}\tilde{\underline{\boldsymbol{d}}}^C \\ &\quad - \hat{\boldsymbol{H}}^{oT}\boldsymbol{O}_{\bar{\boldsymbol{d}}^C}\tilde{\bar{\boldsymbol{d}}}^C - \hat{\boldsymbol{H}}^{oT}\boldsymbol{O}_{\underline{\boldsymbol{t}}^B}\tilde{\underline{\boldsymbol{t}}}^C - \hat{\boldsymbol{H}}^{oT}\boldsymbol{O}_{\bar{\boldsymbol{t}}^C}\tilde{\bar{\boldsymbol{t}}}^C + \boldsymbol{\theta} - \boldsymbol{u}_{\text{rb}} \end{aligned} \tag{47}$$

Theorem 1: The nonlinear 5-D hyper chaotic system given in using (1). The proposed WIT2TFBCC is shown in (31) using the update laws from (48) to (60) combining with the robust controller in (60). Then the robustness of the system can be definite.

$$\dot{\hat{\boldsymbol{H}}}^a = l_{\boldsymbol{H}^a}\boldsymbol{s}^T\hat{\boldsymbol{A}} \tag{48}$$

$$\dot{\hat{\boldsymbol{H}}}^o = l_{\boldsymbol{H}^o}\boldsymbol{s}^T\hat{\boldsymbol{O}} \tag{49}$$

$$\dot{\hat{\underline{t}}}_q^B = l_{\underline{\boldsymbol{t}}^B}s_q\boldsymbol{A}_{\underline{\boldsymbol{t}}_q^B}\hat{\boldsymbol{H}}^a \tag{50}$$

$$\dot{\hat{\bar{t}}}_q^B = l_{\bar{\boldsymbol{t}}^B}s_q\boldsymbol{A}_{\bar{\boldsymbol{t}}_q^B}\hat{\boldsymbol{H}}^a \tag{51}$$

$$\dot{\hat{\underline{t}}}_q^C = -l_{\underline{\boldsymbol{t}}^C}s_q\boldsymbol{O}_{\underline{\boldsymbol{t}}_q^C}\hat{\boldsymbol{H}}^o \tag{52}$$

$$\dot{\hat{\bar{t}}}_q^C = -l_{\bar{\boldsymbol{t}}^C}s_q\boldsymbol{O}_{\bar{\boldsymbol{t}}_q^C}\hat{\boldsymbol{H}}^o \tag{53}$$

$$\dot{\hat{\boldsymbol{m}}}^B = l_{\boldsymbol{m}^B}\boldsymbol{s}\boldsymbol{A}_{\boldsymbol{m}^B}^T\hat{\boldsymbol{H}}^a \tag{54}$$

$$\dot{\hat{\underline{\boldsymbol{d}}}}^B = l_{\underline{\boldsymbol{d}}^B}\boldsymbol{s}\boldsymbol{A}_{\underline{\boldsymbol{d}}^B}^T\hat{\boldsymbol{H}}^a \tag{55}$$

$$\dot{\hat{\bar{\boldsymbol{d}}}}^B = l_{\bar{\boldsymbol{d}}^B}\boldsymbol{s}\boldsymbol{A}_{\bar{\boldsymbol{d}}^B}^T\hat{\boldsymbol{H}}^a \tag{56}$$

$$\dot{\hat{\boldsymbol{m}}}^C = -l_{\boldsymbol{m}^C}\boldsymbol{s}\boldsymbol{O}_{\boldsymbol{m}^C}^T\hat{\boldsymbol{H}}^o \tag{57}$$

$$\dot{\hat{\underline{\boldsymbol{d}}}}^C = -l_{\underline{\boldsymbol{d}}^B}\boldsymbol{s}\boldsymbol{O}_{\underline{\boldsymbol{d}}^C}^T\hat{\boldsymbol{H}}^o \tag{58}$$

$$\dot{\hat{\bar{\boldsymbol{d}}}}^C = -l_{\bar{\boldsymbol{d}}^C}\boldsymbol{s}(t)\boldsymbol{O}_{\bar{\boldsymbol{d}}^B}^T\hat{\boldsymbol{H}}^o \tag{59}$$

$$\boldsymbol{u}_{\text{rb}} = \hat{\boldsymbol{\kappa}}\text{sign}(\boldsymbol{s}) \tag{60}$$

where $l_{\boldsymbol{H}^a}, l_{\boldsymbol{H}^o}, l_{\underline{\boldsymbol{t}}^B}, l_{\bar{\boldsymbol{t}}^B}, l_{\underline{\boldsymbol{t}}^C}, l_{\bar{\boldsymbol{t}}^C}, l_{\boldsymbol{m}^B}, l_{\underline{\boldsymbol{d}}^B}, l_{\bar{\boldsymbol{d}}^B}, l_{\boldsymbol{m}^C}, l_{\underline{\boldsymbol{d}}^C}, l_{\bar{\boldsymbol{d}}^C}$ are learning rates and positive values.

Proof: Defining a Lyapunov function as:

$$\begin{aligned}V &= \boldsymbol{s}^T\boldsymbol{s} + \frac{\tilde{\boldsymbol{H}}^{aT}\tilde{\boldsymbol{H}}^a}{2l_{\boldsymbol{H}^a}} + \frac{\tilde{\boldsymbol{H}}^{oT}\tilde{\boldsymbol{H}}^o}{2l_{\boldsymbol{H}^o}} + \frac{\tilde{\boldsymbol{m}}^{BT}\tilde{\boldsymbol{m}}^B}{2l_{\boldsymbol{m}^B}} + \frac{\tilde{\underline{\boldsymbol{d}}}^{BT}\tilde{\underline{\boldsymbol{d}}}^B}{2l_{\underline{\boldsymbol{d}}^B}} \\ &\quad + \frac{\tilde{\boldsymbol{m}}^{CT}\tilde{\boldsymbol{m}}^C}{l_{\boldsymbol{m}^C}} + \frac{\tilde{\underline{\boldsymbol{d}}}^{CT}\tilde{\underline{\boldsymbol{d}}}^C}{l_{\underline{\boldsymbol{d}}^C}} + \frac{\tilde{\underline{\boldsymbol{t}}}^{BT}\dot{\underline{\boldsymbol{t}}}^B}{l_{\underline{\boldsymbol{t}}^B}} + \frac{\tilde{\bar{\boldsymbol{t}}}^{BT}\dot{\bar{\boldsymbol{t}}}^B}{l_{\bar{\boldsymbol{t}}^B}} + \frac{\tilde{\underline{\boldsymbol{t}}}^{CT}\dot{\underline{\boldsymbol{t}}}^C}{l_{\underline{\boldsymbol{t}}^C}} \\ &\quad + \frac{\tilde{\bar{\boldsymbol{t}}}^{CT}\dot{\bar{\boldsymbol{t}}}^C}{l_{\bar{\boldsymbol{t}}^C}} + \frac{\tilde{\boldsymbol{\kappa}}^2}{2l_\kappa} \end{aligned} \tag{61}$$

where $\tilde{\boldsymbol{\kappa}} = \kappa - \hat{\kappa}$, $\hat{\boldsymbol{\kappa}}$ is the estimation value of $\boldsymbol{\kappa}$ and $\tilde{\boldsymbol{\kappa}}$ is the estimation error.

The derivative of (61) is

$$\begin{aligned}\dot{V} &= \boldsymbol{s}^T\dot{\boldsymbol{s}} + \frac{tr\left(\tilde{\boldsymbol{H}}^{aT}\dot{\tilde{\boldsymbol{H}}}^a\right)}{l_{\boldsymbol{H}^a}} + \frac{tr\left(\tilde{\boldsymbol{H}}^{oT}\dot{\tilde{\boldsymbol{H}}}^o\right)}{l_{\boldsymbol{H}^o}} + \frac{tr\left(\tilde{\underline{\boldsymbol{t}}}^{BT}\dot{\underline{\boldsymbol{t}}}^B\right)}{l_{\underline{\boldsymbol{t}}^B}} \\ &\quad + \frac{tr\left(\tilde{\bar{\boldsymbol{t}}}^{BT}\dot{\bar{\boldsymbol{t}}}^B\right)}{l_{\bar{\boldsymbol{t}}^B}} + \frac{tr\left(\tilde{\underline{\boldsymbol{t}}}^{CT}\dot{\underline{\boldsymbol{t}}}^C\right)}{l_{\underline{\boldsymbol{t}}^C}} + \frac{tr\left(\tilde{\bar{\boldsymbol{t}}}^{CT}\dot{\bar{\boldsymbol{t}}}^C\right)}{l_{\bar{\boldsymbol{t}}^C}} + \frac{\tilde{\boldsymbol{m}}^{BT}\dot{\tilde{\boldsymbol{m}}}^B}{l_{\boldsymbol{m}^B}} \\ &\quad + \frac{\tilde{\underline{\boldsymbol{d}}}^{BT}\dot{\underline{\boldsymbol{d}}}^B}{l_{\underline{\boldsymbol{d}}^B}} + \frac{\tilde{\bar{\boldsymbol{d}}}^{BT}\dot{\bar{\boldsymbol{d}}}^B}{l_{\bar{\boldsymbol{d}}^B}} + \frac{\tilde{\boldsymbol{m}}^{CT}\dot{\tilde{\boldsymbol{m}}}^C}{l_{\boldsymbol{m}^C}} + \frac{\tilde{\underline{\boldsymbol{d}}}^{CT}\dot{\underline{\boldsymbol{d}}}^C}{l_{\underline{\boldsymbol{d}}^C}} \\ &\quad + \frac{\tilde{\bar{\boldsymbol{d}}}^{CT}\dot{\bar{\boldsymbol{d}}}^C}{l_{\bar{\boldsymbol{d}}^C}} + \frac{\tilde{\boldsymbol{\kappa}}\dot{\tilde{\boldsymbol{\kappa}}}}{l_\kappa} \end{aligned} \tag{62}$$

$$\begin{aligned}&= \boldsymbol{s}^T(\hat{\boldsymbol{A}}\tilde{\boldsymbol{H}}^a - \hat{\boldsymbol{O}}\tilde{\boldsymbol{H}}^o + \boldsymbol{A}_{\boldsymbol{m}^B}\tilde{\boldsymbol{m}}^B\hat{\boldsymbol{H}}^a + \boldsymbol{A}_{\underline{\boldsymbol{d}}^B}\tilde{\underline{\boldsymbol{d}}}^B\hat{\boldsymbol{H}}^a + \boldsymbol{A}_{\bar{\boldsymbol{d}}^B}\tilde{\bar{\boldsymbol{d}}}^B\hat{\boldsymbol{H}}^a \\ &\quad + \boldsymbol{A}_{\underline{\boldsymbol{t}}^B}\tilde{\underline{\boldsymbol{t}}}^B\hat{\boldsymbol{H}}^a + \boldsymbol{A}_{\bar{\boldsymbol{t}}^B}\tilde{\bar{\boldsymbol{t}}}^B\hat{\boldsymbol{H}}^a - \boldsymbol{O}_{\boldsymbol{m}^C}\tilde{\boldsymbol{m}}^C\hat{\boldsymbol{H}}^o - \boldsymbol{O}_{\underline{\boldsymbol{d}}^C}\tilde{\underline{\boldsymbol{d}}}^C\hat{\boldsymbol{H}}^o \\ &\quad - \boldsymbol{O}_{\bar{\boldsymbol{d}}^C}\tilde{\bar{\boldsymbol{d}}}^C\hat{\boldsymbol{H}}^o - \boldsymbol{O}_{\underline{\boldsymbol{t}}^B}\tilde{\underline{\boldsymbol{t}}}^C\hat{\boldsymbol{H}}^o - \boldsymbol{O}_{\bar{\boldsymbol{t}}^C}\tilde{\bar{\boldsymbol{t}}}^C\hat{\boldsymbol{H}}^o + \boldsymbol{\theta}(t) - \boldsymbol{u}_{rb}) \\ &\quad + \frac{tr\left(\tilde{\boldsymbol{H}}^{aT}\dot{\tilde{\boldsymbol{H}}}^a\right)}{l_{\boldsymbol{H}^a}} + \frac{tr\left(\tilde{\boldsymbol{H}}^{oT}\dot{\tilde{\boldsymbol{H}}}^o\right)}{l_{\boldsymbol{H}^o}} + \frac{tr\left(\tilde{\underline{\boldsymbol{t}}}^{BT}\dot{\underline{\boldsymbol{t}}}^B\right)}{l_{\underline{\boldsymbol{t}}^B}} \\ &\quad + \frac{tr\left(\tilde{\bar{\boldsymbol{t}}}^{BT}\dot{\bar{\boldsymbol{t}}}^B\right)}{l_{\bar{\boldsymbol{t}}^B}} + \frac{tr\left(\tilde{\underline{\boldsymbol{t}}}^{CT}\dot{\underline{\boldsymbol{t}}}^C\right)}{l_{\underline{\boldsymbol{t}}^C}} + \frac{tr\left(\tilde{\bar{\boldsymbol{t}}}^{CT}\dot{\bar{\boldsymbol{t}}}^C\right)}{l_{\bar{\boldsymbol{t}}^C}} \\ &\quad + \frac{\tilde{\boldsymbol{m}}^{BT}\dot{\tilde{\boldsymbol{m}}}^B}{l_{\boldsymbol{m}^B}} + \frac{\tilde{\underline{\boldsymbol{d}}}^{BT}\dot{\underline{\boldsymbol{d}}}^B}{l_{\underline{\boldsymbol{d}}^B}} + \frac{\tilde{\bar{\boldsymbol{d}}}^{BT}\dot{\bar{\boldsymbol{d}}}^B}{l_{\bar{\boldsymbol{d}}^B}} \\ &\quad + \frac{\tilde{\boldsymbol{m}}^{CT}\tilde{\boldsymbol{m}}^C}{l_{\boldsymbol{m}^C}} + \frac{\tilde{\underline{\boldsymbol{d}}}^{CT}\dot{\underline{\boldsymbol{d}}}^C}{l_{\underline{\boldsymbol{d}}^C}} + \frac{\tilde{\bar{\boldsymbol{d}}}^{CT}\dot{\bar{\boldsymbol{d}}}^C}{l_{\bar{\boldsymbol{d}}^C}} + \frac{\tilde{\boldsymbol{\kappa}}\dot{\tilde{\boldsymbol{\kappa}}}}{l_\kappa} \end{aligned} \tag{63}$$

Remark 1: $\boldsymbol{H}^{a*}$, $\boldsymbol{H}^{o*}$, $\bar{\boldsymbol{t}}^{B*}$, $\bar{\boldsymbol{t}}^{C*}$, $\underline{\boldsymbol{t}}^{B*}$, $\underline{\boldsymbol{t}}^{C*}\boldsymbol{m}^{B*}$, $\boldsymbol{m}^{C*}$, $\underline{\boldsymbol{d}}^{B*}$, $\underline{\boldsymbol{d}}^{C*}$, $\bar{\boldsymbol{d}}^{B*}$, $\bar{\boldsymbol{d}}^{C*}$ are constants, therefore, $\dot{\tilde{\boldsymbol{H}}}^{a} = -\dot{\hat{\boldsymbol{H}}}^{a}$, $\dot{\tilde{\boldsymbol{H}}}^{o} = -\dot{\hat{\boldsymbol{H}}}^{o}$, $\dot{\tilde{\bar{\boldsymbol{t}}}}^{B} = \dot{\hat{\bar{\boldsymbol{t}}}}^{B}$, $\dot{\tilde{\bar{\boldsymbol{t}}}}^{C} = \dot{\hat{\bar{\boldsymbol{t}}}}^{C}$, $\dot{\tilde{\underline{\boldsymbol{t}}}}^{B} = \dot{\hat{\underline{\boldsymbol{t}}}}^{B}$, $\dot{\tilde{\underline{\boldsymbol{t}}}}^{C} = \dot{\hat{\underline{\boldsymbol{t}}}}^{C}$, $\dot{\tilde{\boldsymbol{m}}}^{B} = -\dot{\hat{\boldsymbol{m}}}^{B}$, $\dot{\tilde{\boldsymbol{m}}}^{C} = -\dot{\hat{\boldsymbol{m}}}^{C}$, $\dot{\tilde{\bar{\boldsymbol{d}}}}^{B} = \dot{\hat{\bar{\boldsymbol{d}}}}^{B}$, $\dot{\tilde{\bar{\boldsymbol{d}}}}^{C} = \dot{\hat{\bar{\boldsymbol{d}}}}^{C}$, $\dot{\tilde{\underline{\boldsymbol{d}}}}^{B} = \dot{\hat{\underline{\boldsymbol{d}}}}^{B}$, $\dot{\tilde{\underline{\boldsymbol{d}}}}^{C} = \dot{\hat{\underline{\boldsymbol{d}}}}^{C}$.

Remark 2:

$$\begin{cases} \hat{\boldsymbol{H}}^{aT}\boldsymbol{A}_{\boldsymbol{m}^B}\tilde{\boldsymbol{m}}^{B} = \tilde{\boldsymbol{m}}^{BT}\boldsymbol{A}^{T}_{\boldsymbol{m}^B}\hat{\boldsymbol{H}}^{a} \\ \hat{\boldsymbol{H}}^{aT}\boldsymbol{A}_{\underline{\boldsymbol{d}}^B}\tilde{\underline{\boldsymbol{d}}}^{B} = \tilde{\underline{\boldsymbol{d}}}^{BT}\boldsymbol{A}^{T}_{\underline{\boldsymbol{d}}^B}\hat{\boldsymbol{H}}^{a} \\ \hat{\boldsymbol{H}}^{aT}\boldsymbol{A}_{\bar{\boldsymbol{d}}^B}\tilde{\bar{\boldsymbol{d}}}^{B} = \tilde{\bar{\boldsymbol{d}}}^{BT}\boldsymbol{A}^{T}_{\bar{\boldsymbol{d}}^B}\hat{\boldsymbol{H}}^{a} \\ \hat{\boldsymbol{H}}^{oT}\boldsymbol{O}_{\boldsymbol{m}^C}\tilde{\boldsymbol{m}}^{C} = \tilde{\boldsymbol{m}}^{CT}\boldsymbol{O}^{T}_{\boldsymbol{m}^C}\hat{\boldsymbol{H}}^{o} \\ \hat{\boldsymbol{H}}^{oT}\boldsymbol{O}_{\underline{\boldsymbol{d}}^C}\tilde{\underline{\boldsymbol{d}}}^{C} = \tilde{\underline{\boldsymbol{d}}}^{CT}\boldsymbol{O}^{T}_{\underline{\boldsymbol{d}}^C}\hat{\boldsymbol{H}}^{o} \\ \hat{\boldsymbol{H}}^{oT}\boldsymbol{O}_{\bar{\boldsymbol{d}}^C}\tilde{\bar{\boldsymbol{d}}}^{C} = \tilde{\bar{\boldsymbol{d}}}^{CT}\boldsymbol{O}^{T}_{\bar{\boldsymbol{d}}^C}\hat{\boldsymbol{H}}^{o} \end{cases}$$

and

$$\begin{cases} tr\left(\tilde{\boldsymbol{H}}^{aT}\dot{\hat{\boldsymbol{H}}}^{a}\right) = \sum_{q=1}^{n_q}\tilde{\boldsymbol{H}}^{aT}\dot{\hat{\boldsymbol{H}}}^{a} \\ tr\left(\tilde{\boldsymbol{H}}^{oT}\dot{\hat{\boldsymbol{H}}}^{o}\right) = \sum_{q=1}^{n_q}\tilde{\boldsymbol{H}}^{oT}\dot{\hat{\boldsymbol{H}}}^{o} \\ tr\left(\tilde{\underline{\boldsymbol{t}}}^{BT}\dot{\hat{\underline{\boldsymbol{t}}}}^{B}\right) = \sum_{q=1}^{n_q}\tilde{\underline{t}}_q^{BT}\dot{\hat{\underline{t}}}_q^{B} \\ tr\left(\tilde{\bar{\boldsymbol{t}}}^{BT}\dot{\hat{\bar{\boldsymbol{t}}}}^{B}\right) = \sum_{q=1}^{n_q}\tilde{\bar{t}}_q^{BT}\dot{\hat{\bar{t}}}_q^{B} \\ tr\left(\tilde{\underline{\boldsymbol{t}}}^{CT}\dot{\hat{\underline{\boldsymbol{t}}}}^{C}\right) = \sum_{q=1}^{n_q}\tilde{\underline{t}}_q^{CT}\dot{\hat{\underline{t}}}_q^{C} \\ tr\left(\tilde{\bar{\boldsymbol{t}}}^{CT}\dot{\hat{\bar{\boldsymbol{t}}}}^{C}\right) = \sum_{q=1}^{n_q}\tilde{\bar{t}}_q^{CT}\dot{\hat{\bar{t}}}_q^{C} \end{cases}$$

$$\begin{aligned} \dot{V} = &\sum_{q=1}^{n_q}\tilde{\boldsymbol{H}}^{aT}\left(\boldsymbol{s}^{T}.\hat{\boldsymbol{A}} - \frac{\dot{\hat{\boldsymbol{H}}}^{a}}{l_{H^a}}\right) \\ &- \sum_{q=1}^{n_q}\tilde{\boldsymbol{H}}^{oT}\left(\boldsymbol{s}^{T}.\hat{\boldsymbol{O}} + \frac{\dot{\hat{\boldsymbol{H}}}^{o}}{l_{H^o}}\right) \\ &+ \sum_{q=1}^{n_q}\tilde{\underline{t}}_q^{BT}\left(s_q.\boldsymbol{A}_{\underline{t}_q^B}\hat{\boldsymbol{H}}^{a} - \frac{\dot{\hat{\underline{t}}}_q^{B}}{l_{\underline{t}^B}}\right) \\ &+ \sum_{q=1}^{n_q}\tilde{\bar{t}}_q^{BT}\left(s_q.\boldsymbol{A}_{\bar{t}_q^B}\hat{\boldsymbol{H}}^{a} - \frac{\dot{\hat{\bar{t}}}_q^{B}}{l_{\bar{t}^B}}\right) \\ &- \sum_{q=1}^{n_q}\tilde{\underline{t}}_q^{CT}\left(s_q.\boldsymbol{O}_{\underline{t}_q^C}\hat{\boldsymbol{H}}^{o} + \frac{\dot{\hat{\underline{t}}}_q^{C}}{l_{\underline{t}^C}}\right) \\ &- \sum_{q=1}^{n_q}\tilde{\bar{t}}_q^{CT}\left(s_q.\boldsymbol{O}_{\bar{t}_q^C}\hat{\boldsymbol{H}}^{o} + \frac{\dot{\hat{\bar{t}}}_q^{C}}{l_{\bar{t}^B}}\right) \\ &+ \tilde{\boldsymbol{m}}^{BT}\left(\boldsymbol{s}.\boldsymbol{A}^{T}_{\boldsymbol{m}^B}\hat{\boldsymbol{H}}^{a} - \frac{\dot{\hat{\boldsymbol{m}}}^{B}}{l_{\boldsymbol{m}^B}}\right) + \tilde{\underline{\boldsymbol{d}}}^{BT}\left(\boldsymbol{s}.\boldsymbol{A}^{T}_{\underline{\boldsymbol{d}}^B}\hat{\boldsymbol{H}}^{a} - \frac{\dot{\hat{\underline{\boldsymbol{d}}}}^{B}}{l_{\bar{\boldsymbol{d}}^B}}\right) + \tilde{\bar{\boldsymbol{d}}}^{BT} \\ &\times\left(\boldsymbol{s}.\boldsymbol{A}^{T}_{\bar{\boldsymbol{d}}^B}\hat{\boldsymbol{H}}^{a} - \frac{\dot{\hat{\bar{\boldsymbol{d}}}}^{B}}{l_{\bar{\boldsymbol{d}}^B}}\right) \end{aligned}$$

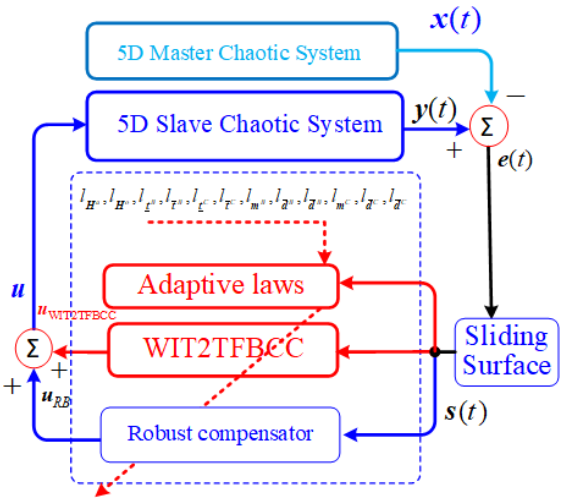

FIGURE 2. The structure of the proposed synchronization method.

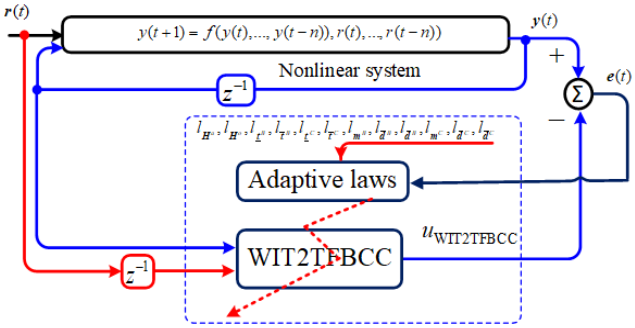

FIGURE 3. The structure of nonlinear system prediction using proposed WIT2TFBCC.

$$\begin{aligned} &-\tilde{\boldsymbol{m}}^{CT}\left(\boldsymbol{s}.\boldsymbol{O}^{T}_{\boldsymbol{m}^C}\hat{\boldsymbol{H}}^{o} + \frac{\dot{\hat{\boldsymbol{m}}}^{C}}{l_{\boldsymbol{m}^C}}\right) - \tilde{\underline{\boldsymbol{d}}}^{CT}\left(\boldsymbol{s}.\boldsymbol{O}^{T}_{\underline{\boldsymbol{d}}^C}\hat{\boldsymbol{H}}^{o} + \frac{\dot{\hat{\underline{\boldsymbol{d}}}}^{C}}{l_{\bar{\boldsymbol{d}}^B}}\right) \\ &-\tilde{\bar{\boldsymbol{d}}}^{BT}\left(\boldsymbol{s}.\boldsymbol{O}^{T}_{\bar{\boldsymbol{d}}^B}\hat{\boldsymbol{H}}^{o} + \frac{\dot{\hat{\bar{\boldsymbol{d}}}}^{C}}{l_{\bar{\boldsymbol{d}}^C}}\right) + \boldsymbol{s}^{T}\left(\theta - \boldsymbol{u}_{rb}\right) + \frac{\tilde{\boldsymbol{\kappa}}\dot{\tilde{\boldsymbol{\kappa}}}}{l_{\kappa}} \end{aligned} \tag{64}$$

Via the compensator in (60) and the update parameters in (43)-(54), (64) becomes:

$$\begin{aligned} \dot{V} &= \boldsymbol{s}^{T}(\boldsymbol{\theta} - \boldsymbol{u}_{\mathrm{rb}}) + \frac{\tilde{\boldsymbol{\kappa}}\dot{\tilde{\boldsymbol{\kappa}}}}{l_{\kappa}} = \boldsymbol{s}^{T}\left(\boldsymbol{\theta} - \hat{\boldsymbol{\kappa}}sign(\boldsymbol{s})\right) + \frac{\tilde{\boldsymbol{\kappa}}\dot{\tilde{\boldsymbol{\kappa}}}}{l_{\kappa}} \\ &= \boldsymbol{s}^{T}\boldsymbol{\theta} - \hat{\boldsymbol{\kappa}}\left\|\boldsymbol{s}\right\| + \frac{\tilde{\boldsymbol{\kappa}}\dot{\tilde{\boldsymbol{\kappa}}}}{l_{\kappa}} \end{aligned} \tag{65}$$

If the adaptive law of the error bound is adjusted by as below: $\dot{\tilde{\boldsymbol{\kappa}}} = -\dot{\hat{\boldsymbol{\kappa}}} = -l_{\kappa}\left\|\boldsymbol{s}\right\|$, then (65) becomes

$$\begin{aligned} \dot{V} &= \boldsymbol{s}^{T}\boldsymbol{\theta} - \hat{\boldsymbol{\kappa}}\left\|\boldsymbol{s}\right\| - \left(\boldsymbol{\kappa} - \hat{\boldsymbol{\kappa}}\right)\left\|\boldsymbol{s}\right\| = \boldsymbol{s}^{T}\boldsymbol{\theta} - \boldsymbol{\kappa}\left\|\boldsymbol{s}\right\| \\ &\leq \left\|\boldsymbol{\theta}\right\|.\left\|\boldsymbol{s}\right\| - \boldsymbol{\kappa}\left\|\boldsymbol{s}\right\| \\ &= -\left(\boldsymbol{\kappa} - \left\|\boldsymbol{\theta}\right\|\right)\left\|\boldsymbol{s}\right\| \leq 0 \end{aligned} \tag{66}$$

Since $\dot{V}(k)$ is negative semi-definite, it shows that $\tilde{\boldsymbol{\kappa}}$ and $\boldsymbol{s}(t)$ are bounded. Define $\Gamma = \left(\boldsymbol{\kappa} - \left\|\boldsymbol{\theta}\right\|\right)\boldsymbol{s} \leq \left(\boldsymbol{\kappa} - \left\|\boldsymbol{\theta}\right\|\right).\left\|\boldsymbol{s}\right\| \leq -\dot{V}$. Integrating Γ with admiration to

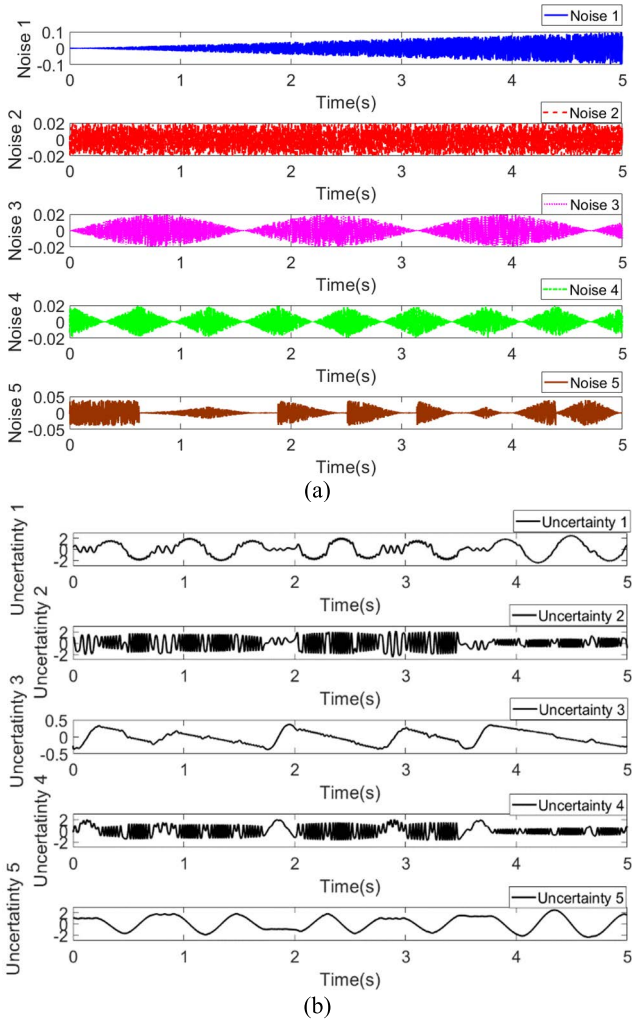

FIGURE 4. **(a) The external pertubations, and (b) uncertainties of 5D chaotic system.**

time, obtains:

$$\int_0^t \Gamma(\varsigma)d\varsigma \leq V(0) - V(t) \tag{67}$$

Because $V(0)$ is bounded, $\dot{V}$ does not increase and bounded, so $\lim_{t\to\infty} \int_0^t \Gamma(\varsigma)d\varsigma < \infty$. This indicates that when $t \to \infty$ then $s \to 0$. Therefore, the stability for the proposed WIT2TFBCC algorithm is proved.

III. THE WIT2FBCC PARAMETER LEARNING ALGORITHM FOR TIME SERIES PREDICTION

Consider a nonlinear system described as [1]

$$y(t+1) = f(y(t), y(t-1), \ldots, y(t-n)), r(t), r(t-1), \ldots, r(t-n)) \tag{68}$$

where $f(.)$ is the unknown function $f : \Re^n \to \Re$, r and y are the input and output of the system, respectively. The input data $r(t)$ is used to train the network and the final output from the neural network is also the output of the system.

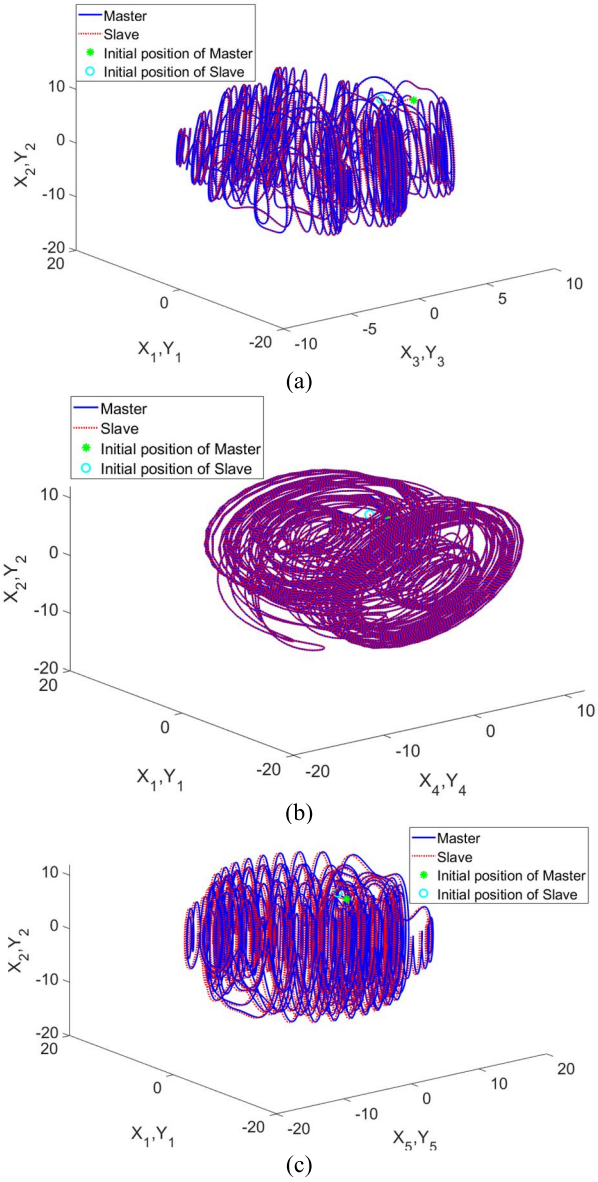

FIGURE 5. **3D projection of 5D chaotic system (a) $x_1x_2x_3$, (b) $x_1x_2x_4$, and (c) $x_1x_2x_5$.**

Considering the single input-single output system for simplicity, the tracking error for the system is defined as

$$e(t) = y(t) - y_N(t) \tag{69}$$

where $y_N(t)$ is the desired output for the system and $y_N(t) = u_{\text{WIT2TFBCC}}(t)$ is the output of the neural network.

A. CONVERGENCE ANALYSIS FOR CHAOS TIME-SERIES PREDICTION

A Lyapunov function is given as follows:

$$V_p(t) = \frac{1}{2}e^2(t) \tag{70}$$

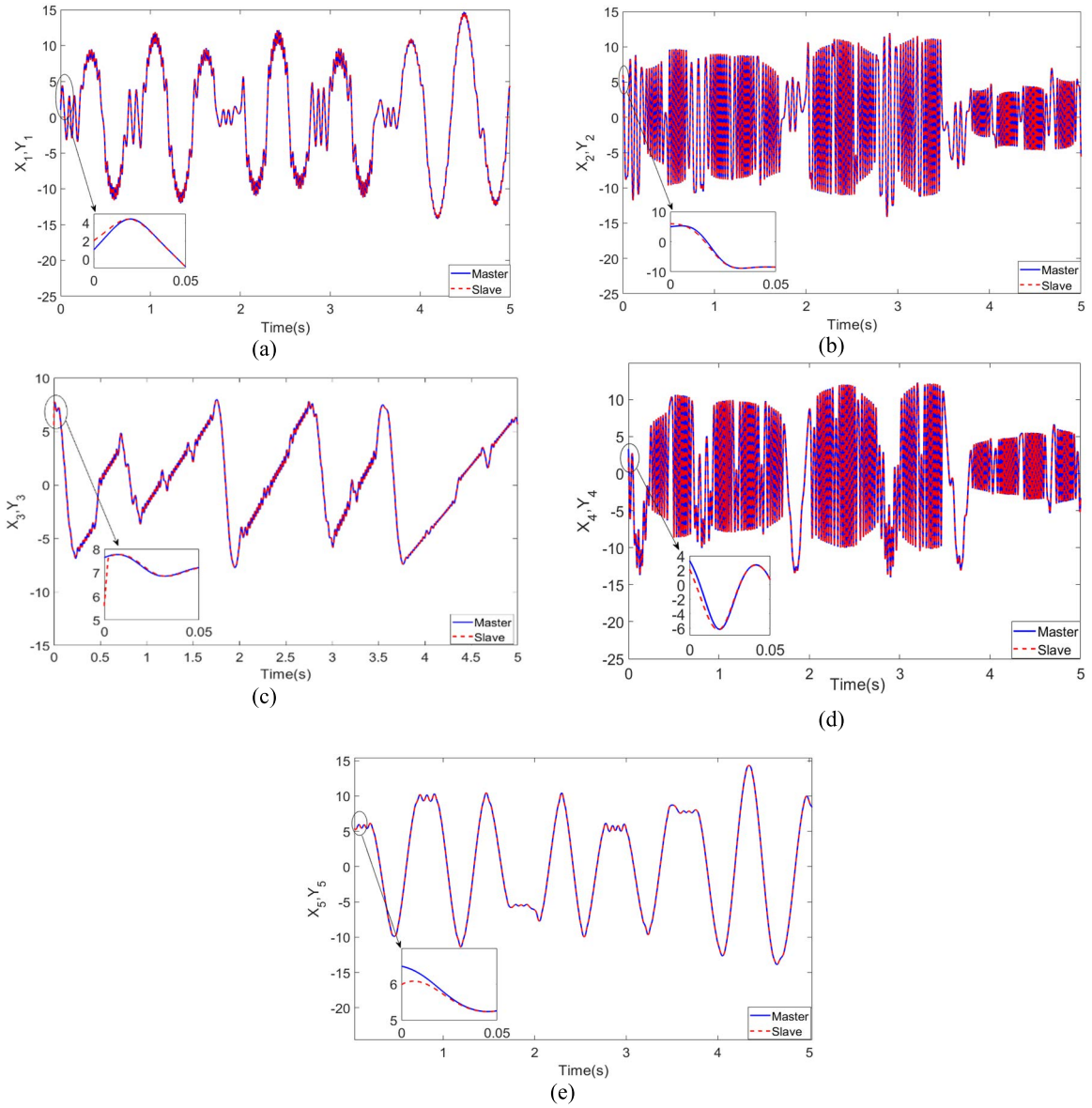

FIGURE 6. The Synchronization of each axis of 5D chaotic system using WIT2TFBCC (a) x_1y_1, (b) x_2y_2, (c) x_3y_3, (d) x_4y_4 and (e) x_5y_5.

The derivate of V:

$$\Delta V_p(t) = V_p(t+1) - V_p(t) = \frac{1}{2}(e^2(t+1) - e^2(t)) \quad (71)$$

According to the literature [19], the error can be represented by

$$e(t+1) = e(t) - \Delta e(t) \cong e(t) + \left(\frac{\partial e(t)}{\partial \Upsilon}\right)^T \Delta\Upsilon \quad (72)$$

where $\Delta\Upsilon$ is the change of Υ. from (12) to (13), obtains

$$\Delta\Upsilon = l_\Upsilon \left(-\frac{\partial E_\Upsilon(t)}{\partial \Upsilon}\right) = l_\Upsilon e_\Upsilon(t)\frac{\partial \hat{y}(t)}{\partial \Upsilon} \quad (73)$$

where l_Z can be one of these learning rates $l_{\boldsymbol{H}^a}$, $l_{\boldsymbol{H}^o}$, $l_{\underline{\boldsymbol{t}}^B}$, $l_{\bar{\boldsymbol{t}}^B}$, $l_{\underline{\boldsymbol{t}}^C}$, $l_{\bar{\boldsymbol{t}}^C}$, $l_{\boldsymbol{m}^B}$, $l_{\bar{\boldsymbol{d}}^B}$, $l_{\bar{\boldsymbol{d}}^B}$, $l_{\boldsymbol{m}^C}$, $l_{\bar{\boldsymbol{d}}^C}$, $l_{\bar{\boldsymbol{d}}^C}$. Thus,

$$\begin{aligned}
\Delta V_p(t) &= \frac{1}{2}\left(e^2(t+1) - e^2(t)\right) \\
&= \frac{1}{2}(e(t+1) - e(t))(e(t+1) + e(t)) \\
&= \frac{1}{2}\Delta e(t)\left[e(t) + \frac{1}{2}\Delta e(t)\right] \\
&= \left[\frac{\partial e(t)}{\partial \Upsilon}\right]^T l_\Upsilon e(t)\frac{\partial \hat{y}(t)}{\partial \Upsilon} \\
&\quad \times \left[e(t) + \frac{1}{2}\left(\frac{\partial e(t)}{\partial \Upsilon}\right)^T l_\Upsilon e(t)\frac{\partial \hat{y}(t)}{\partial \Upsilon}\right]
\end{aligned}$$

TABLE 2. The parameters of 5D hyper chaotic system.

The parameter systems	$a_1=30,\ a_2=30,\ a_3=10,\ a_4=30$
The uncertainties	$\Delta \boldsymbol{f}(\boldsymbol{y}_S)=rands(.)\left[0.2y_1,\ 0.2y_2,\ 0.2y_3,\ 0.2y_4,\ 0.2y_5\right]^T$
The initial condition states	$\boldsymbol{x}(0)=\left[0.8,\ 4.9,\ 7.6,\ 3.7,\ 6.5\right]^T$, $\boldsymbol{y}(0)=\left[1.8,\ 5.9,\ 5.6,\ 2.65,\ 6\right]^T$
The external pertubations	$\boldsymbol{n}(t)=rands(.)\times \begin{bmatrix} 0.02\times t \\ 0.02\times square(5\times t) \\ 0.03\times \sin(2\times t) \\ 0.02\times sawtooth(10\times t) \\ 0.02\times (square(5\times t)+\cos(t^2)) \end{bmatrix}$

TABLE 3. Initial parameters of the proposed WIT2TFBCC.

	WIT2TFBELC	WIT2TFCMAC
Total of blocks for associative domain	5	5
The block number of receptive field domain	-	5
The block number of weight memory domain	5	5
Number of sub-output domain	2	2
The initialization range for centers m_{iq}^B and m_{iq}^C	[−0.2, 0.2]	[−0.2, 0.2]
Initial upper variances $\overline{d}_{iq}^B$ and $\overline{d}_{iq}^C$	0.005	0.005
Initial lower variances $\underline{d}_{iq}^B$ and $\underline{d}_{iq}^C$	0.005	0.0005
The initialization range for $\overline{t}_{iq}^B$ and $\overline{t}_{iq}^C$	[−0.5, 0.5]	[−0.5, 0.5]
The initialization range for $\underline{t}_{iq}^B$ and $\underline{t}_{iq}^C$	[−0.5, 0.5]	[−0.5, 0.5]
Learning rates for l_{H^a}, and l_{H^o}	0.005	0.005
Learning rates for TSK $l_{\underline{t}^B}, l_{\overline{t}^B}$, and $l_{\underline{t}^C}, l_{\overline{t}^C}$	0.002, 0.002	0.002, 0.002
Learning-rate for $l_{m^B}, l_{\overline{d}^B}, l_{\underline{d}^B}$, and $l_{m^C}, l_{\overline{d}^C}, l_{\underline{d}^C}$	0.0001, 0.0001, 0.0001	0.001, 0.001, 0.001
Learning-rate of robust compensator l_κ	0.01	0.01

TABLE 4. Comparison in root mean square error (RMSE) of WIT2TFBCC and other methods.

Method	Computation Time (ms)	RMSE1	RMSE2	RMSE3	RMSE4	RMSE5	Average _RMSE
CMAC	0.15	0.0111	0.0111	0.2648	0.0105	0.2251	0.1047
RNN [36]	0.16	0.0090	0.0061	0.1916	0.0057	0.2703	0.0965
TSKCMAC [35]	0.17	0.0076	0.0039	0.1499	0.0036	0.3038	0.0938
BELC	0.18	0.0066	0.0027	0.1227	0.0026	0.33293	0.093506
RCFBC	0.20	0.0052	0.0016	0.0894	0.0015	0.3751	0.0946
T2FBELC [18]	0.205	0.0047	0.0013	0.0790	0.0016	0.3815	0.0936
DFLFBEC [13]	0.21	0.0061	0.0020	0.1211	0.0020	0.3264	0.0915
Our method	0.22	0.0040	0.0010	0.0532	0.0010	0.3977	0.0914

$$= -\left[\frac{\partial \hat{y}(t)}{\partial \Upsilon}\right]^T l_\Upsilon e(t)\frac{\partial \hat{y}(t)}{\partial \Upsilon} \times \left[e(t)-\frac{1}{2}\left(\frac{\partial e(t)}{\partial \Upsilon}\right)^T l_z e(t)\frac{\partial \hat{y}(t)}{\partial \Upsilon}\right] = -l_\Upsilon e(t)\left|\frac{\partial \hat{y}(t)}{\partial \Upsilon}\right|^2\left[1-\frac{1}{2}l_\Upsilon\left|\frac{\partial \hat{y}(t)}{\partial \Upsilon}\right|^2\right] \quad (74)$$

Let The term Z_Υ is the variable that represents for the expression $Z_\Upsilon = \frac{\partial \hat{y}(t)}{\partial \Upsilon}$, gives

$$\Delta V_p(t) = -\beta_\Upsilon e^2(t)\left|Z_\Upsilon(t)\right|^2\left[1-\frac{1}{2}l_\Upsilon\left(Z_\Upsilon(t)\right)^2\right] \quad (75)$$

If l_z is chosen as

$$0 < l_z < \frac{2}{(\max(Z_\Upsilon))^2} \quad (76)$$

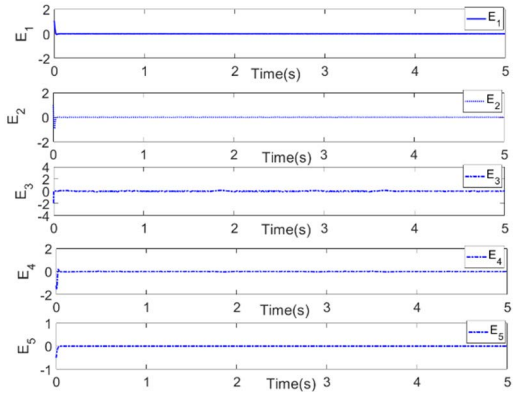

FIGURE 7. The error signal of each axis of 5D chaotic system using WIT2TFBCC.

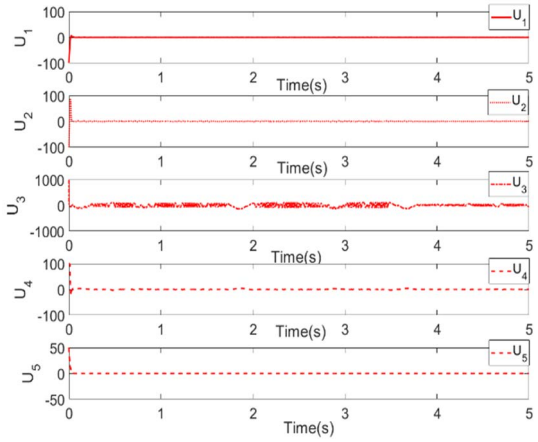

FIGURE 8. The control signal of each axis of 5D chaotic system using WIT2TFBCC.

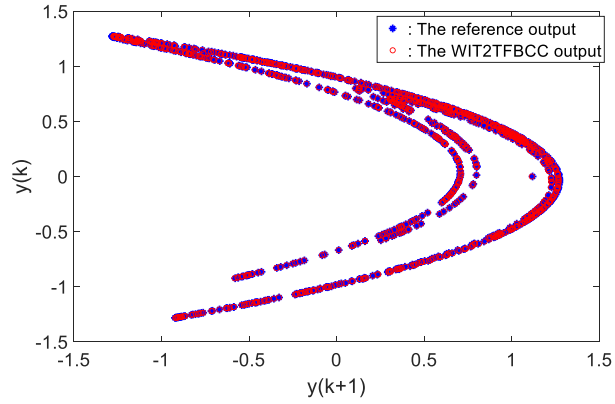

FIGURE 9. Phase plane plot of reference output and predicted output for Henon map chaotic system.

Therefore, $\frac{1}{2}l_\Upsilon\,(Z_\Upsilon(t))^2 \leq 1$, so $\Delta V_p(t) < 0$. Thus, the convergence of the online learning algorithm is guaranteed by the Lyapunov stability theorem in Section II. The error between the desired output and the output of the WIT2TFBCC converges to zero if $t \to \infty$.

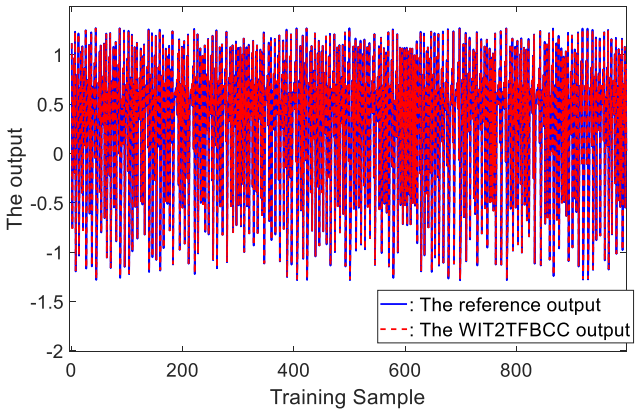

FIGURE 10. Result of training process using the proposed WIT2TFBCC.

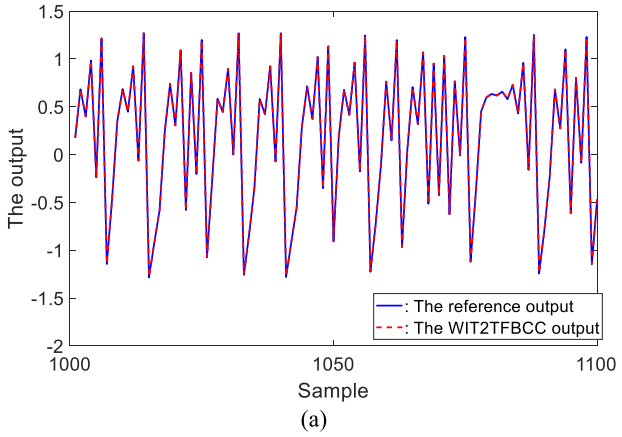

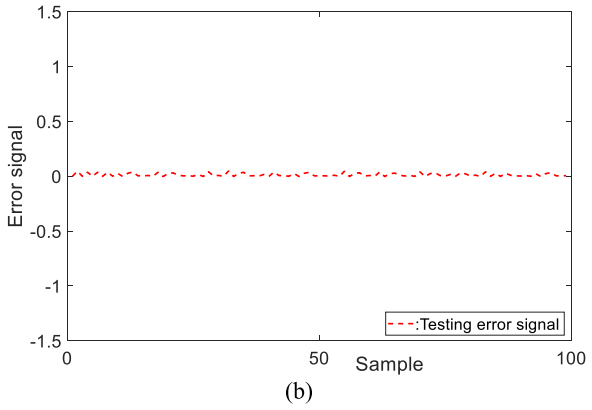

FIGURE 11. (a) The testing output with 100 samples, and (b) The error signal of the testing process using the proposed WIT2TFBCC.

IV. WIT2TFBCC FOR 5-D HYPERCHAOTIC SYNCHRONIZATION

The parameters of the 5D hyper chaotic system are given in Table 5. where *rand*(·) builds a random number in range [0, 1]. The parameters for the proposed WIT2TFBCC control system are selected for WIT2TFBCC, the parameters of the proposed WIT2TFBCC are shown in Table 2.

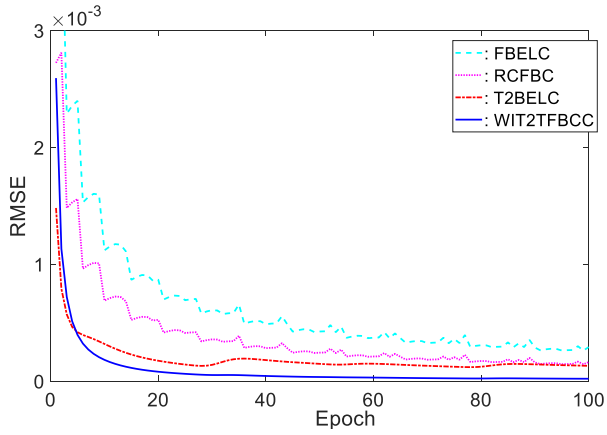

FIGURE 12. RMSE using the proposed WIT2TFBCC during 100 epochs.

The external perturbations and uncertainties of the hyperchaotic system are shown in Figs. 4(a) and (b), respectively. The 3D projections of the synchronization for the 5D hyperchaotic system using the WIT2TFBCC are shown in Fig. 5, and the synchronization of each axis is shown in Fig. 6. The tracking errors are shown in Fig. 7, and the control effort is shown in Fig. 8. From the simulation results, the proposed method synchronizes well with small tracking errors. In particular, the average RMSE of WIT2TFBCC is reduced and reaches the smallest value among all (see Table 4). However, WIT2TFBCC requires longer computation time due to its complex structure. This is reasonable because the higher the performance, the larger the computational cost.

The external perturbations and uncertainties of the hyperchaotic system are shown in Figs. 4(a) and (b), respectively. The 3D projections of the synchronization for the 5D hyperchaotic system using the WIT2TFBCC are shown in Fig. 5, and the synchronization of each axis is shown in Fig. 6. The tracking errors are shown in Fig. 7, and the control effort is shown in Fig. 8. From the simulation results, the proposed method synchronizes well with small tracking errors. In particular, the average RMSE of WIT2TFBCC is reduced and reaches the smallest value among all (see Table 4). However, WIT2TFBCC requires longer computation time due to its complex structure. This is reasonable because the higher the performance, the larger the computational cost.

V. SIMULATION RESULTS OF WIT2TFBCC FOR HENON MAP TIME SERIES PREDICTION

Our method can be applied to the prediction of time series systems such as Henon map time series to illustrate the performance of our method. The Henon map is chosen as the prediction plant, which is referred to as [1] and [7]:

$$y(k+1) = -1.4y^2(k) + 0.3y(k-1) + 1 \qquad (77)$$

This system has the past input-output values $y(k)$, $y(k-1)$ therefore a parallel model is needed for the time series prediction. 1000 data points are chosen from the system over the interval $[-1.51.5]$. The initial conditions are defined as $y(0) = y(1) = 0.4$. Next, we use the training architecture for chaos time series prediction in Fig. 9, which shows the reference output and the predicted output of training and test data for the chaotic Henon map system. Fig. 10 shows the training process with 1000 samples between the blue solid line (the reference output) and the red dotted line (the output prediction with WIT2TFBCC). Fig. 11 (a) shows the testing process with 100 samples and Fig. 11(b) shows the result of the error signal between the reference output and the prediction output with our method. Fig. 12 shows the RMSE between our method and the others FBELC, RCFBC and T2BELC, the RMSE of our method is the best among them all because it converges to zero faster and more elastic. Table 5 shows the comparison of our method with the others, the test RMSE of our method is the smallest among all, but the calculation time is the longest because of the complexity of our method.

TABLE 5. Comparison of proposed method with others.

Methods	Computation time (ms)	Testing RMSE
WTFCMNN [7]	--	0.0186
FBELC	10.75	0.0245
RCFBC [12]	11.85	0.0234
T2BELC	17.23	0.0217
WIT2TFBCC	18.45	0.0128

VI. CONCLUSION

In this study, the method for designing the WIT2TFBCC controller for synchronizing chaotic systems and predicting time series is proposed. The proposed controller has been successfully tested for synchronization of 5-D hyperchaotic systems and prediction of Henon Map time series. For the convergence of the chaotic synchronization system, an additional compensator with the sign function is used due to the complexity of the chaotic system. However, for the prediction of time series, no compensator is used, only optimal convergence according to the learning rate must be used, since the time series change continuously with time. Future studies can be 1) using optimal algorithms, such as modified grey wolf optimization (MGWO), to find the optimal learning rates faster, 2) applying our method for hardware applications.

REFERENCES

[1] C. H. Lee, F. Y. Chang, and C. M. Lin, "An efficient interval type-2 fuzzy CMAC for chaos time-series prediction and synchronization," *IEEE Trans. Cybern.*, vol. 44, no. 3, pp. 329–341, Mar. 2014.

[2] Z. Wang, L. Li, M. Song, J. Yan, J. Shi, and Y. Yao, "Evaluating the traditional Chinese medicine (TCM) officially recommended in China for COVID-19 using ontology-based side-effect prediction framework (OSPF) and deep learning," *J. Ethnopharmacol.*, vol. 272, May 2021, Art. no. 113957.

[3] W. Chen, H. Xu, L. Jia, and Y. Gao, "Machine learning model for bitcoin exchange rate prediction using economic and technology determinants," *Int. J. Forecasting*, vol. 37, no. 1, pp. 28–43, Jan. 2021.
[4] N. Shatnawi and H. Abu-Qdais, "Assessing and predicting air quality in northern Jordan during the lockdown due to the COVID-19 virus pandemic using artificial neural network," *Air Qual., Atmos. Health*, vol. 14, no. 5, pp. 643–652, May 2021.
[5] X. Li, Z. Han, T. Zhao, J. Zhang, and D. Xue, "Modeling for indoor temperature prediction based on time-delay and Elman neural network in air conditioning system," *J. Building Eng.*, vol. 33, Jan. 2021, Art. no. 101854.
[6] K. Elbaz, S.-L. Shen, A. Zhou, Z.-Y. Yin, and H.-M. Lyu, "Prediction of disc cutter life during shield tunneling with AI via the incorporation of a genetic algorithm into a GMDH-type neural network," *Engineering*, vol. 7, no. 2, pp. 238–251, Feb. 2021.
[7] J. Zhao and C.-M. Lin, "Wavelet-TSK-type fuzzy cerebellar model neural network for uncertain nonlinear systems," *IEEE Trans. Fuzzy Syst.*, vol. 27, no. 3, pp. 549–558, Mar. 2019.
[8] R. Chandra, S. Goyal, and R. Gupta, "Evaluation of deep learning models for multi-step ahead time series prediction," *IEEE Access*, vol. 9, pp. 83105–83123, 2021.
[9] X. Li, F. Bi, X. Yang, and X. Bi, "An echo state network with improved topology for time series prediction," *IEEE Sensors J.*, vol. 22, no. 6, pp. 5869–5878, Mar. 2022.
[10] V. N. Giap, Q. D. Nguyen, and S. C. Huang, "Synthetic adaptive fuzzy disturbance observer and sliding-mode control for chaos-based secure communication systems," *IEEE Access*, vol. 9, pp. 23907–23928, 2021.
[11] N. V. Giap, H. S. Vu, Q. D. Nguyen, and S.-C. Huang, "Disturbance and uncertainty rejection-based on fixed-time sliding-mode control for the secure communication of chaotic systems," *IEEE Access*, vol. 9, pp. 133663–133685, 2021.
[12] C.-M. Lin, D.-H. Pham, and T.-T. Huynh, "Synchronization of chaotic system using a brain-imitated neural network controller and its applications for secure communications," *IEEE Access*, vol. 9, pp. 75923–75944, 2021.
[13] H.-. T. Tu, C.-M. Lin, D.-H. Pham, N.-. P. Nguyen, N. Q.-K. Le, V.-P. Vu, and F. Chao, "4-D memristive chaotic systems-based audio secure communication using dual-function-link fuzzy brain emotional controller," *Int. J. Fuzzy Syst.*, vol. 24, pp. 2946–2968, May 2022.
[14] C.-M. Lin, D.-H. Pham, and T.-T. Huynh, "Encryption and decryption of audio signal and image secure communications using chaotic system synchronization control by TSK fuzzy brain emotional learning controllers," *IEEE Trans. Cybern.*, early access, Dec. 22, 2021, doi: 10.1109/TCYB.2021.3134245.
[15] T.-L. Le, "Multilayer interval type-2 fuzzy controller design for hyperchaotic synchronization," *IEEE Access*, vol. 9, pp. 155286–155296, 2021.
[16] K. M. Hosny, S. T. Kamal, and M. M. Darwish, "Novel encryption for color images using fractional-order hyperchaotic system," *J. Ambient Intell. Humanized Comput.*, vol. 13, pp. 973–988, Jan. 2022.
[17] S. Yan, Q. Wang, E. Wang, X. Sun, and Z. Song, "Multi-scroll fractional-order chaotic system and finite-time synchronization," *Phys. Scripta*, vol. 97, no. 2, Feb. 2022, Art. no. 025203.
[18] T.-L. Le, C.-M. Lin, and T.-T. Huynh, "Self-evolving type-2 fuzzy brain emotional learning control design for chaotic systems using PSO," *Appl. Soft Comput.*, vol. 73, pp. 418–433, Dec. 2018.
[19] T.-T. Huynh, C.-M. Lin, T.-L. Le, N. P. Nguyen, S.-K. Hong, and F. Chao, "Wavelet interval type-2 fuzzy quad-function-link brain emotional control algorithm for the synchronization of 3D nonlinear chaotic systems," *Int. J. Fuzzy Syst.*, vol. 22, no. 8, pp. 2546–2564, Nov. 2020.
[20] V.-N. Giap, S.-C. Huang, and Q. D. Nguyen, "Synchronization of 3D chaotic system based on sliding mode control: Electronic circuit implementation," in *Proc. IEEE Eurasia Conf. IoT, Commun. Eng. (ECICE)*, Oct. 2020, pp. 156–159.
[21] Z. Deng, Y. Jiang, K.-S. Choi, F.-L. Chung, and S. Wang, "Knowledge-leverage-based TSK fuzzy system modeling," *IEEE Trans. Neural Netw. Learn. Syst.*, vol. 24, no. 8, pp. 1200–1212, Aug. 2013.
[22] T.-T. Huynh, T.-L. Le, and C.-M. Lin, "Self-organizing recurrent wavelet fuzzy neural network-based control system design for MIMO uncertain nonlinear systems using TOPSIS method," *Int. J. Fuzzy Syst.*, vol. 21, no. 2, pp. 468–487, Mar. 2019.
[23] T.-L. Le, T.-T. Huynh, and S.-K. Hong, "Self-organizing interval type-2 fuzzy asymmetric CMAC design to synchronize chaotic satellite systems using a modified grey wolf optimizer," *IEEE Access*, vol. 8, pp. 53697–53709, 2020.
[24] T.-T. Huynh, C.-M. Lin, and T.-L. Le, "A double function-link function-based fuzzy brain emotional controller for synchronizing a 4D hyperchaotic system," in *Proc. IEEE Int. Conf. Syst., Man, Cybern. (SMC)*, Oct. 2020, pp. 1961–1965.
[25] C. Lucas, D. Shahmirzadi, and N. Sheikholeslami, "Introducing BELBIC: Brain emotional learning based intelligent controller," *Intell. Autom. Soft Comput.*, vol. 10, no. 1, pp. 11–21, Jan. 2004.
[26] S. Bicakci, "On the implementation of fuzzy VMC for an under actuated system," *IEEE Access*, vol. 7, pp. 163578–163588, 2019.
[27] X. Jiang, S. Li, B. Luo, and Q. Meng, "Source exploration for an under-actuated system: A control-theoretic paradigm," *IEEE Trans. Control Syst. Technol.*, vol. 28, no. 3, pp. 1100–1107, May 2020.
[28] M. Lutter, K. Listmann, and J. Peters, "Deep Lagrangian networks for end-to-end learning of energy-based control for under-actuated systems," in *Proc. IEEE/RSJ Int. Conf. Intell. Robots Syst. (IROS)*, Nov. 2019, pp. 7718–7725.
[29] S. Vaidyanathan, A. Sambas, B. Abd-El-Atty, A. A. A. El-Latif, E. Tlelo-Cuautle, O. Guillen-Fernandez, M. Mamat, M. A. Mohamed, M. Alcin, M. Tuna, I. Pehlivan, I. Koyuncu, and M. A. H. Ibrahim, "A 5-D multi-stable hyperchaotic two-disk dynamo system with no equilibrium point: Circuit design, FPGA realization and applications to TRNGs and image encryption," *IEEE Access*, vol. 9, pp. 81352–81369, 2021.
[30] F. Chao, D. Zhou, C.-M. Lin, L. Yang, C. Zhou, and C. Shang, "Type-2 fuzzy hybrid controller network for robotic systems," *IEEE Trans. Cybern.*, vol. 50, no. 8, pp. 3778–3792, Aug. 2020.
[31] M. M. Zirkohi, "Adaptive interval type-2 fuzzy recurrent RBFNN control design using ellipsoidal membership functions with application to MEMS gyroscope," *ISA Trans.*, vol. 119, pp. 25–40, Jan. 2022.
[32] C.-H. Chiu and C.-Y. Wu, "Bicycle robot balance control based on a robust intelligent controller," *IEEE Access*, vol. 8, pp. 84837–84849, 2020.
[33] J. Zhang, F. Chao, H. Zeng, C.-M. Lin, and L. Yang, "A recurrent wavelet-based brain emotional learning network controller for nonlinear systems," *Soft Comput.*, vol. 26, no. 6, pp. 3013–3028, Mar. 2022.
[34] S.-Y. Wang, C.-M. Lin, and C.-H. Li, "Design of adaptive TSK fuzzy self-organizing recurrent cerebellar model articulation controller for chaotic systems control," *Appl. Sci.*, vol. 11, no. 4, p. 1567, Feb. 2021.
[35] C.-M. Lin and H.-Y. Li, "TSK fuzzy CMAC-based robust adaptive backstepping control for uncertain nonlinear systems," *IEEE Trans. Fuzzy Syst.*, vol. 20, no. 6, pp. 1147–1154, Dec. 2012.
[36] C.-H. Lee and C.-C. Teng, "Identification and control of dynamic systems using recurrent fuzzy neural networks," *IEEE Trans. Fuzzy Syst.*, vol. 8, no. 4, pp. 349–366, Aug. 2000.

DUC-HUNG PHAM was born in Hung Yen, Vietnam, in 1983. He received the B.S. degree in automatic control and the M.S. degree in automation from the Hanoi University of Science and Technology, Vietnam, in 2006 and 2011, respectively, and the Ph.D. degree from the Department of Electrical Engineering, Yuan Ze University, Chung-Li, Taiwan, in 2022. He is currently a Lecturer with the Faculty Electrical and Electronic, Hung Yen University of Technical and Education, Vietnam. His research interests include fuzzy logic control, neural networks, cerebellar model articulation controller, brain emotional learning-based intelligent controller, and secure communication.

CHIH-MIN LIN (Fellow, IEEE) was born in Changhua, Taiwan, in 1959. He received the B.S. and M.S. degrees from the Department of Control Engineering, National Chiao Tung University, Hsinchu, Taiwan, in 1981 and 1983, respectively, and the Ph.D. degree from the Institute of Electronics Engineering, National Chiao Tung University, in 1986. He is currently a Chair Professor of Yuan Ze University, Taoyuan, Taiwan. He also serves as an Associate Editor for IEEE TRANSACTIONS ON CYBERNETICS and IEEE TRANSACTIONS ON FUZZY SYSTEMS. From 1997 to 1998, he was the Honor Research Fellow at the University of Auckland, New Zealand. He has published more than 200 journal articles and 160 conference papers. His research interests include fuzzy neural networks, cerebellar model articulation controller, intelligent control systems, adaptive signal processing, and classification problem.

VAN NAM GIAP received the B.S. degree in control engineering and automation from the Ha Noi University of Science and Technology, Hanoi, Vietnam, in 2015, the master's degree in electronic engineering from the National Kaohsiung University of Applied and Sciences, Kaohsiung, Taiwan, in 2017, and the Ph.D. degree in mechanical engineering from the National Kaohsiung University of Science and Technology, Taiwan, in June 2021. He is currently with the Hanoi University of Science and Technology, Vietnam. His research interests include sliding mode control, disturbance and uncertainty estimation, fuzzy logic control, secure communication, the magnetic bearing system and its applications, and self-bearing motors.

TUAN-TU HUYNH (Member, IEEE) was born in Ho Chi Minh City, Vietnam, in 1982. He received the B.S. degree in electrical & electronics from the Department of Electrical & Electronics Engineering, Ho Chi Minh University of Technology and Education, Vietnam, in 2005, the M.S. degree in automation from the Ho Chi Minh City University of Transport, Vietnam, in 2010, and the Ph.D. degree in electrical engineering from Yuan Ze University, Chung-Li, Taoyuan, Taiwan, in 2018. He is currently a Research Fellow with the Department of Electrical Engineering, Yuan Ze University. He is also a Lecturer with the Faculty of Mechatronics and Electronics, Lac Hong University, Vietnam. His research interests include MCDM, fuzzy logic control, neural networks, cerebellar model articulation controller, brain emotional learning-based intelligent controller, deep learning, and intelligent control systems.

HSING-YUEH CHO was born in Taiwan, in 1989. He received the master's degree in electrical engineering from the Chien Hsin University of Science and Technology, Zhongli, Taiwan, in 2013. He is currently pursuing the Ph.D. degree in electrical engineering with Yuan Ze University, Taoyuan.

His research interests include fuzzy logic control, adaptive control, cerebellar model articulation controllers, and intelligent control systems.